SCIENCE CHINA
Chemistry

•REVIEWS•
SPECIAL TOPIC: Rechargeable Battery Technology

January 2024 Vol.67 No.1: 67–86
https://doi.org/10.1007/s11426-023-1866-y

A review of solid-state lithium metal batteries through *in-situ* solidification

Pan Xu[1], Zong-Yao Shuang[1], Chen-Zi Zhao[1*], Xue Li[2], Li-Zhen Fan[3], Aibing Chen[4], Haoting Chen[5], Elena Kuzmina[6], Elena Karaseva[6], Vladimir Kolosnitsyn[6], Xiaoyuan Zeng[2], Peng Dong[2], Yingjie Zhang[2], Mingpei Wang[5] & Qiang Zhang[1,7,8*]

[1]*Beijing Key Laboratory of Green Chemical Reaction Engineering and Technology, Department of Chemical Engineering, Tsinghua University, Beijing 100084, China;*
[2]*National and Local Joint Engineering Laboratory for Lithium-ion Batteries and Materials Preparation Technology, Key Laboratory of Advanced Battery Materials of Yunnan Province, Faculty of Metallurgical and Energy Engineering, Kunming University of Science and Technology, Kunming 650093, China;*
[3]*Institute of Advanced Materials and Technology, University of Science and Technology Beijing, Beijing 100083, China;*
[4]*College of Chemical and Pharmaceutical Engineering, Hebei University of Science and Technology, Shijiazhuang 050018, China;*
[5]*Ordos Carbon Neutral Research and Application Co., Ltd., Ordos City 017010, China;*
[6]*Ufa Institute of Chemistry UFRC RAS, Ufa 450054, Russia;*
[7]*Institute for Carbon Neutrality, Tsinghua University, Beijing 100084, China;*
[8]*Shanxi Research Institute for Clean Energy, Tsinghua University, Taiyuan 030032, China*

Received October 5, 2023; accepted October 30, 2023; published online November 2, 2023

High-energy-density lithium metal batteries are the next-generation battery systems of choice, and replacing the flammable liquid electrolyte with a polymer solid-state electrolyte is a prominent conduct towards realizing the goal of high-safety and high-specific-energy devices. Unfortunately, the inherent intractable problems of poor solid–solid contacts between the electrode/electrolyte and the growth of Li dendrites hinder their practical applications. The *in-situ* solidification has demonstrated a variety of advantages in the application of polymer electrolytes and artificial interphase, including the design of integrated polymer electrolytes and asymmetric polymer electrolytes to enhance the compatibility of solid–solid contact and compatibility between various electrolytes, and the construction of artificial interphase between the Li anode and cathode to suppress the formation of Li dendrites and to enhance the high-voltage stability of polymer electrolytes. This review firstly elaborates the history of *in-situ* solidification for solid-state batteries, and then focuses on the synthetic methods of solidified electrolytes. Furthermore, the recent progress of *in-situ* solidification technology from both the design of polymer electrolytes and the construction of artificial interphase is summarized, and the importance of *in-situ* solidification technology in enhancing safety is emphasized. Finally, prospects, emerging challenges, and practical applications of *in-situ* solidification are envisioned.

***in-situ* solidification, polymer electrolyte, artificial solid electrolyte interphase, rechargeable lithium metal batteries, dendrite-free lithium metal anode**

Citation: Xu P, Shuang ZY, Zhao CZ, Li X, Fan LZ, Chen A, Chen H, Kuzmina E, Karaseva E, Kolosnitsyn V, Zeng X, Dong P, Zhang Y, Wang M, Zhang Q. A review of solid-state lithium metal batteries through *in-situ* solidification. *Sci China Chem*, 2024, 67: 67–86, https://doi.org/10.1007/s11426-023-1866-y

*Corresponding authors (email: zcz@mail.tsinghua.edu.cn; zhang-qiang@mails.tsinghua.edu.cn)

1 Introduction

The development of human society has been inextricably linked to energy, and now we have ushered in the fourth wave of the "new energy" revolution. Encouragingly, in 2019, the Nobel Prize in Chemistry was awarded to John B. Goodenough, M. Stanley Whittingham, and Akira Yoshino, in recognition of their pioneering contributions to lithium-ion batteries (LIBs) [1–12]. Currently, graphite is often used as the anode material in commercialized lithium-ion batteries (LIBs), and its theoretical specific capacity is about 372 mAh g^{-1}. However, due to the insertion/extraction mechanism of lithium ions, the energy density of LIBs is difficult to break through the 350 Wh kg^{-1} and is close to the theoretical limit by compounding graphite with cathodes with lower theoretical specific capacity [13–20], which is difficult to fulfill the rapid development of transportation electrification such as portable electronic devices and new energy vehicles. On this account, the development of high-energy-density and high-safety electrochemical energy storage systems has been strongly considered [21–30].

As the "holy grail" of anode materials, metallic lithium (Li) has numerous advantages of an ultra-high theoretical specific capacity of 3,860 mAh g^{-1}, a low electrode potential of −3.04 V (*vs*. standard hydrogen electrode), and a low density of 0.534 g cm^{-3}, when matched with high-capacity, ternary, lithium-rich manganese-based cathode, it is expected to realize a high-energy-density greater than 500 Wh kg^{-1} [31–42], and thus lithium metal batteries (LMBs) are an excellent choice for the next generation of high specific energy batteries. Nonetheless, the poor adaptability of conventional liquid electrolyte (LE) LMBs, their susceptibility to safety accidents such as combustion and explosion, as well as the uncontrollable dendritic growth at high cycling capacity, hindered their widespread application [43–60]. Notably, solid-state LMBs, the core of which revolves around the solid-state electrolyte can render a high-energy-density, wide operating temperature, long cycling lifetime, and high-safety energy devices. Therefore, the application of solid-state electrolytes instead of organic liquid electrolytes is a practical strategy to achieve safe LMBs [61–74].

Currently, solid-state electrolytes are divided into inorganic/polymer/composite solid-state electrolytes [75–86]. Among them, inorganic solid-state electrolytes are often dominated by oxide, sulfide, and halide electrolytes, which possess advantages such as the high ionic conductivity and wide electrochemical window, but face many challenges such as cumbersome processing, high brittleness, and high impedance at the solid–solid interface of assembled batteries [87–102]. The polymer-based solid-state electrolytes with impressive flexibility and processability are strongly considered. Among them, PEO-based polymer electrolytes are the most considered due to the excellent ionic transport of ether-based chain segments (–O–CH_2–CH_2–O–), but their fatal drawback is the poor anti-oxidation (<4.0 V), which significantly limits their application in high-voltage LMBs [103–111]. Moreover, although unsaturated carbonate olefins have strong anti-oxidation after polymerization, ion transport is limited [112–120]. In view of this point, the key to constructing high-performance solid-state LMBs is that the polymer solid-state electrolyte needs to comply with both high ionic conductivity and high-voltage resistance. Consequently, composite solid-state electrolytes based on polymer electrolytes are proposed and fabricated by means of blending, plasticization and addition of inorganic fillers, *etc.* [121–130]. Although composite solid-state electrolytes have made some progress in improving ionic conductivity, oxidation resistance, mechanical stability, and lithium anode compatibility at room temperature, most of the polymer solid-state electrolyte and composite solid-state electrolyte still adopt the conventional solution casting and other *ex-situ* solidification methods to prepare solid-state electrolyte films [131,132]. There is large impedance between the electrode/electrolyte interfaces of solid-state batteries assembled with above solid-state electrolyte films, resulting in a large electrochemical polarization, and it is hard to exhibit an excellent electrochemical performance. Especially, when matched with high areal loading cathodes, the poor solid–solid contacts of interface become more prominent due to the higher pore number between the electrode particles. In addition, the loose solid–solid contacts cannot resist the dendrite growth, and the interphase of Li anodes is susceptible to fragmentation during the high-capacity lithium plating/stripping process. As solutions to these problems, *in-situ* solidification technology can render a fast ion-transport pathway between the electrode/electrode and electrode/electrolyte, achieve the effective contacts between the electrode/electrolyte interfaces, reduce the interfacial impedance, and improve the electrochemical performance. A stable and robust interphase on the lithium anode surface can be pre-constructed through the *in-situ* solidification technique, which is more compact than the interphase formed by the *ex-situ* solidification, and can regulate the behavior of lithium plating and inhibit the growth of dendrites (Figure 1). On this account, the *ex-situ* solidification technique mainly refers to the pre-construction of the electrolyte film outside the battery independently of the electrodes, while the *in-situ* solidification technique mainly refers to the integration of the electrolyte and electrodes outside or inside the battery to form the film. Markedly, solid-state batteries based on the *in-situ* solidification technology have been strongly considered [133–140].

This review addresses the safety of high-energy-density LMBs as an entry point, expounds the importance of *in-situ* solidification in improving safety and adaptability as well as the history of the development of *in-situ* solidification, and emphatically introduces the synthesis techniques of *in-situ*

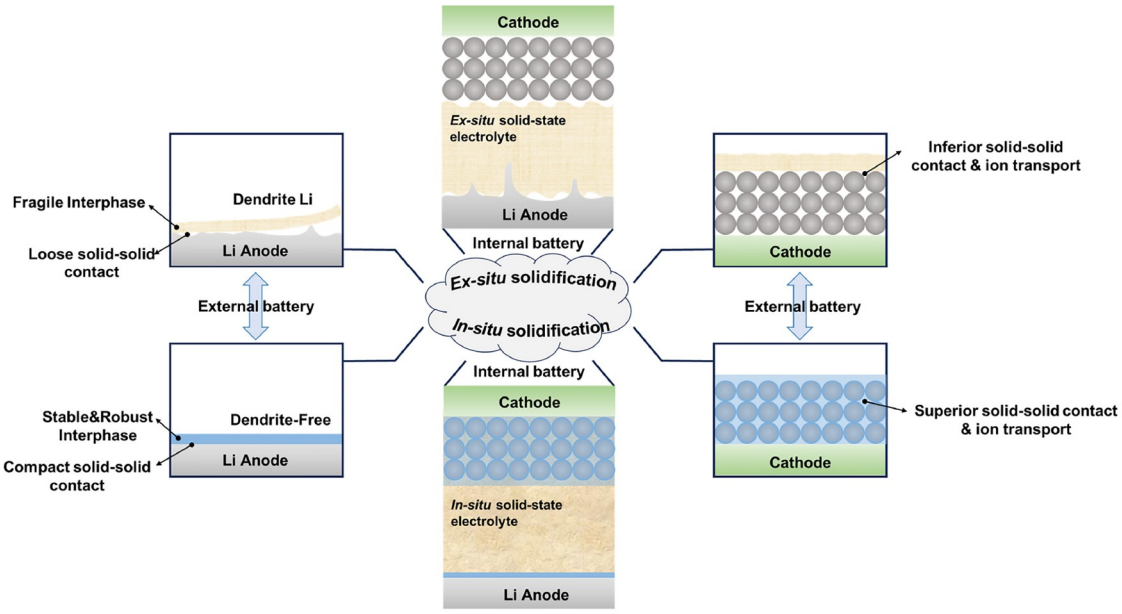

Figure 1 Schematic illustration of external/internal batteries with *ex-situ* solidification and *in-situ* solidification (color online).

solidified polymer electrolyte. The practicalization of *in-situ* solidification technology is promoted from the aspects of artificial interphase construction and polymer electrolyte design, respectively, which clarify and establish the importance of the *in-situ* solidification technology in the development of high-performance and high-safety LMBs. Eventually, the design, challenges and application prospects of the *in-situ* solidified polymer electrolyte are presented to promote the development of existing energy technologies.

2 The *in-situ* solidification of solid-state batteries

The effect of *in-situ* solidification in the design of electrode materials and polymer electrolytes is remarkable for battery communities. Throughout the development of *in-situ* solidification, researchers envisioned preventing leakage by solidified electrolytes as early as the 1800s, and in the 1830s, Michael Faraday [141] discovered ionic conduction properties in solids for the first time. In the 1880s, Carl Gassner [23] introduced the concept of "electrolyte jellification" to improve Leclanche cell. Afterwards, researchers adopted cellulosic materials (*e.g.*, sawdust), bio/natural polymer-based soluble thickeners (*e.g.*, starch, agar paste), simple cloth or starch-coated paper as the separator to further improve the Leclanche cells [142]. Until 1970s, Dey [143] discovered that a passivation layer formed on the surface of highly active lithium metal when immersed in an organic electrolyte, and this phenomenon was investigated in detail by Peled *et al*. in 1979, naming the passivation layer as solid electrolyte interphase (SEI), and they found that SEI can effectively resist the side reaction between the electrolyte and metallic lithium [144,145], which also provides a guiding idea for the preparation of a stable artificial interphase with the help of the *in-situ* solidification to play its role at the present time. In the same period, Exxon pioneered the first viable secondary lithium battery in the 1970s [146]. However, it did not last long, due to the rampant growth of dendrites in liquid LMBs, resulting in short-circuiting and even explosion of the battery, and was thus gradually hidden in the market. Until the 1990s, Sony launched the LIBs [146]. Their positive and negative electrodes were based on lithium iron phosphate ($LiFePO_4$), lithium cobalt ($LiCoO_2$) and graphite, respectively, which have excellent stability and have been utilized until now. Recently, with the rapid development of the new energy field, routine liquid LIBs have been difficult to meet the demand for extended range (>1,000 km), accompanied by numerous fire, explosion, and other safety accidents caused by the liquid electrolyte leakage. As a result, the high-energy-density LMBs are strongly considered again, looking forward to the combination of solid-state electrolytes to achieve high-performance and high-safety of LMBs. To achieve this goal, Deiseroth *et al*. [147] discovered a novel Li_6PS_5X inorganic solid-state electrolyte with ultra-high Li-ion mobility in 2008, and since then various high-performance inorganic solid-state electrolytes such as LGPS and LSPSC have been reported [148,149]. Remarkably, in the 2017, Hu *et al*. [150] prepared a solid-state electrolyte with a three-dimensional (3D) bilayer garnet structure, which successfully promoted the development of solid-state lithium–sulfur batteries and

significantly improved the safety of LMBs. Nonetheless, no matter how researchers compounded two or more kinds of inorganic solid-state electrolytes, they found that the solid-state electrolytes were not only cumbersome and costly to be prepared, but also difficult to solve the intractable issue of poor solid–solid interface contacts. Later, polymer electrolytes have been widely concerned because of their simple preparation process, low-cost, good mechanical properties and toughness, but initially it was still hard to tackle the solid–state interface contact problem by adopting the *ex-situ* strategies to construct polymer electrolyte films. On this basis, it is worth noting that the *in-situ* solidification technology can realize superior solid–solid interface contacts between electrode materials and polymer electrolytes, and construct fast ion-transport pathways, therefore highlighting the importance of the *in-situ* solidification technology.

The *in-situ* solidified polymer electrolytes are produced by selecting active monomers (unsaturated double bonds and cyclic ether monomers) to be solidified outside and inside the battery by various synthetic methods such as free radical polymerization and ionic polymerization (Figure 1). They can be categorized into solid polymer electrolytes (SPE), gel polymer electrolytes (GPE), and composite polymer electrolytes (CPE). Among them, SPE is the earliest class of polymer electrolytes researched, and so far, the ionic conductivity of the vast majority of SPE is relatively low, but the electrochemical stability and the stability of the electrode is good; GPE, as a transition product between liquid electrolytes and all solid-state electrolytes, combines the flexibility of solid and the ease diffusion of liquid; CPE is based on the polymer electrolyte as the main body by adding suitable fillers, such as inorganic solid-state electrolyte can not only enhance the mechanical properties of the polymer electrolyte, but also promote the ionic conductivity. Notably, in 2018 and 2019, Guo and Archer [151,152] adopted cationic polymerization to prepare polymer 1,3-dioxocyclopentane (pDOL) electrolytes by *in-situ* solidifying 1,3-dioxocyclopentane (DOL) solvent inside the battery, demonstrating the potential of multi-system adaptation, which once again set off a research boom in PEO-based electrolytes. However, although the ionic conductivity of PEO-based electrolytes is high, they have poor oxidation resistance and cannot be matched with high-voltage cathode materials. Conversely, polymer electrolytes from the polymerization of unsaturated carbonate-based olefinic monomers exhibit high-voltage resistance but low ionic conductivity. In view of this, on the basis of *in-situ* solidification, researchers have found that the introduction of plasticizers or synergistic compounding of PEO-based and polycarbonate-based electrolytes can lead to the preparation of polymer electrolytes with an excellent combination of high ionic conductivity and high-voltage resistance. Furthermore, the *in-situ* solidification technique can pre-construct a stable polymer electrolyte interphase on the electrode surface, participate in and regulate the formation of SEI/CEI, and thus significantly improve the plating/stripping behavior of Li and enhance the high-voltage stability of the polymer electrolytes. Therefore, in-depth research on *in-situ* solidified polymer electrolytes is expected to culminate in the practical application of LMBs (Figure 2).

3 The *in-situ* solidified polymer electrolyte techniques

The synthesis of *in-situ* solidified polymer electrolytes is an ionic conductor produced by the polymerization of different monomers under certain conditions, and the reaction mechanism depends on the reactive groups of the organic monomers and the initiating conditions. Currently, the common polymerization reaction mechanism is dominated by the free-radical polymerization, ionic polymerization, and other polymerizations (initiator-free gamma-ray, electrochemical polymerization, gel factor polymerization, *etc*.) [23,153–158]. Among them, free-radical polymerization and ionic polymerization are often applied to the design of electrode materials and polymer electrolytes by the *in-situ* solidification to optimize battery performance.

3.1 Free radical polymerization

Free radical polymerization is the most commonly used synthetic method to synthesize polymer electrolytes, in which free radicals, as initiators of the reaction, are often generated by the modulation of the external environment (heating, ultraviolet light, microwave, high-energy irradiation, *etc*.) and plasma initiation, and these free radicals can easily react with reactive monomers to form an initiator, free-radical chain, which can further interact with other reactive monomers to achieve chain growth and polymerization. Finally, the polymerization is terminated by the introduction of a capping agent or depletion of the reactive monomers. In the battery system, an appropriate amount of free radical initiators are added to the electrolyte formulation to realize the *in-situ* solidification of electrode materials and polymer electrolyte by adjusting the reaction temperature outside or inside the battery. Generally, the free radical polymerization reaction can be divided into uncontrolled free radical (UFR) polymerization and controlled free radical (CFR) polymerization according to the activity of the radical chain.

3.1.1 Uncontrolled free radical polymerization

UFR polymerization often utilizes peroxides (*e.g*., benzoyl peroxide (BPO), *etc*.), azo compounds (*e.g*., azodiisobutyric acid dimethyl ester (AIBME) and azodiisobutyronitrile (AIBN), *etc*.) as initiators [132]. The polymerization of unsaturated bonded olefin monomers (acrylates, vinylidene

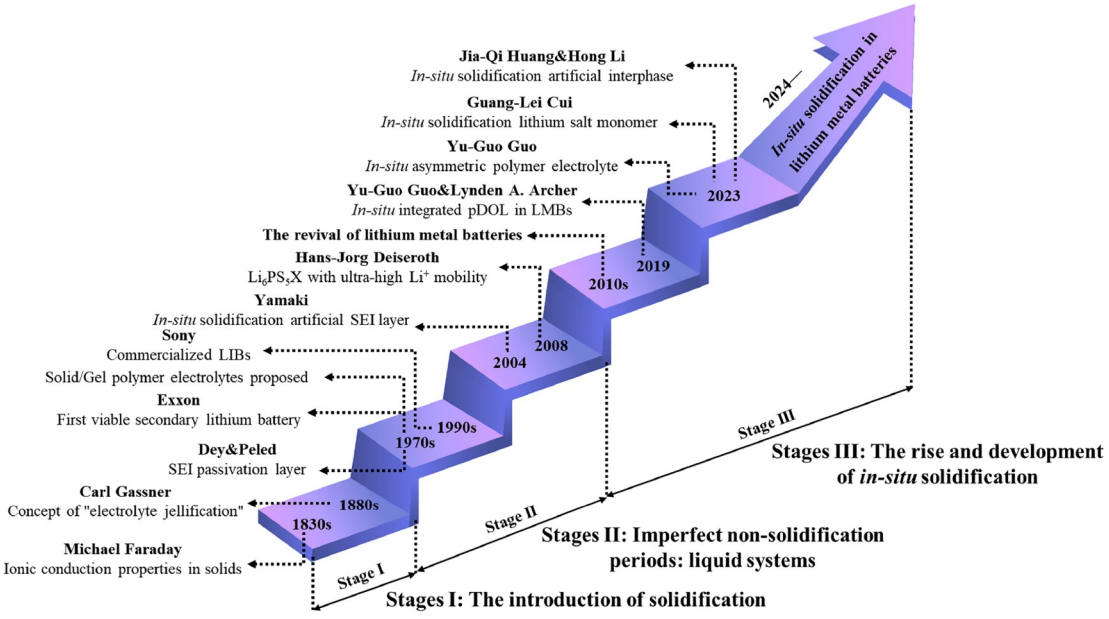

Figure 2 A brief chronology of the development of *in-situ* solidification. The timeline shows the key developments from 1830s to the present. Reproduced with permission Ref. [141]. Copyright 2017, Nature Publication Group; Reproduced with permission Ref. [23]. Copyright 2021, the Royal Society of Chemistry; Reproduced with permission Ref. [61,143,144]. Copyright 2020, 1977, 1979, The Electrochemical Society; Reproduced with permission Ref. [145]. Copyright 2016, Wiley-VCH; Reproduced with permission Ref. [146]. Reproduced with permission Ref. [205]. Copyright 2004, The Electrochemical Society; Copyright 2018, Wiley-VCH; Reproduced with permission Ref. [147]. Copyright 2008, Wiley-VCH; Reproduced with permission Ref. [150]. Copyright 2017, the Royal Society of Chemistry; Reproduced with permission Ref. [151]. Copyright 2018, American Association for the Advancement of Science; Reproduced with permission Ref. [152]. Copyright 2019, Nature publication group; Reproduced with permission Ref. [170]. Copyright 2023, the Royal Society of Chemistry; Reproduced with permission Ref. [198]. Copyright 2023, Wiley-VCH; Reproduced with permission Ref. [203]. Copyright 2023, Nature Publication Group; Reproduced with permission Ref. [207]. Copyright 2022, Elsevier B. V. (color online).

carbonate, *etc*.), which is widely studied nowadays, belongs to UFR polymerization, in which linear or cross-linked polymers are formed by designing the molecular structure of the monomers. Meanwhile, the functional groups (*e.g*., cyano groups, perfluoro groups) are introduced to broaden the electrochemical window and facilitate the migration of lithium ions, thereby optimizing the overall properties of polymer electrolytes.

Recently, Tan *et al*. [159] adopted 2,2′-azobis(2-methylpropionitrile) as the initiator and vinylidene carbonate (VC) as the monomer to obtain the polymer electrolyte (PVC) by the *in-situ* free radical polymerization reaction at 45 °C, achieving high ionic conductivity (4.4 mS cm^{-1}), high Young's modulus (12.4 GPa), high Li^+ mobility number (0.76), and wide electrochemical window (0–4.9 V *vs*. Li^+/Li), effectively suppressing the formation of dendrites and the occurrence of side reactions. As expected, the assembled full-cell (Li||$LiNi_{0.8}Co_{0.1}Mn_{0.1}O_2$) performed the capacity retention up to 87.7% after 200 cycles. More notably, the *in-situ* encapsulation of triethyl phosphate (TEP) into polycarbonate matrix enhances the flame-retardant properties of the system, which in turn demonstrates higher safety in Ah-grade pouch batteries (Figure 3a). On this basis, Lin *et al*. [160] employed vinyl ethylene carbonate (VEC), a monomer similar to VC, as a monomer to produce pVEC by the *in-situ* solidified method. In the pVEC system, lithium ions are transported rapidly (2.1 mS cm^{-1}) through coupling/decoupling interactions with O atoms on the C=O and C–O groups, and the Li||$LiFePO_4$ battery can deliver a high discharge capacity of 104 mAh g^{-1} at −15 °C. In 2022, Sun *et al*. [161] produced poly(vinyl ferrocene) (PVF) with a uniform distribution of iron element by the free radical polymerization applying AIBN as the initiator and metal-based vinyl ferrocene as the monomer. They found that Li^+ and anion can be used together as charge carriers, which significantly enhances the ionic conductivity, and the assembled Li||PVF battery can perform a discharge specific capacity of up to 108 mAh g^{-1} at a current density of 100 μA cm^{-2}, and a stable cycling of 4,000 cycles at a current density of 300 μA cm^{-2}. In order to construct single-ionic polymerized electrolytes, Cao *et al*. [162] used maleic anhydride and lithium 4-styrenesulfonyl(phenyl-sulfonyl)imide in a simple free radical copolymerization reaction under the action of AIBN initiator to produce a new type of single-ionic conductors with the alternating structure, which was composited with poly(vinylidene fluoride-hexafluoropropylene) to produce a SPE membrane. Impressively, the ionic conductivity and Li^+ transfer number of the SPE membrane can be as high as 2.67 mS cm^{-1} and 0.98 at room temperature (25 °C). Based on a methacrylate-based polymer matrix induced by the thermal

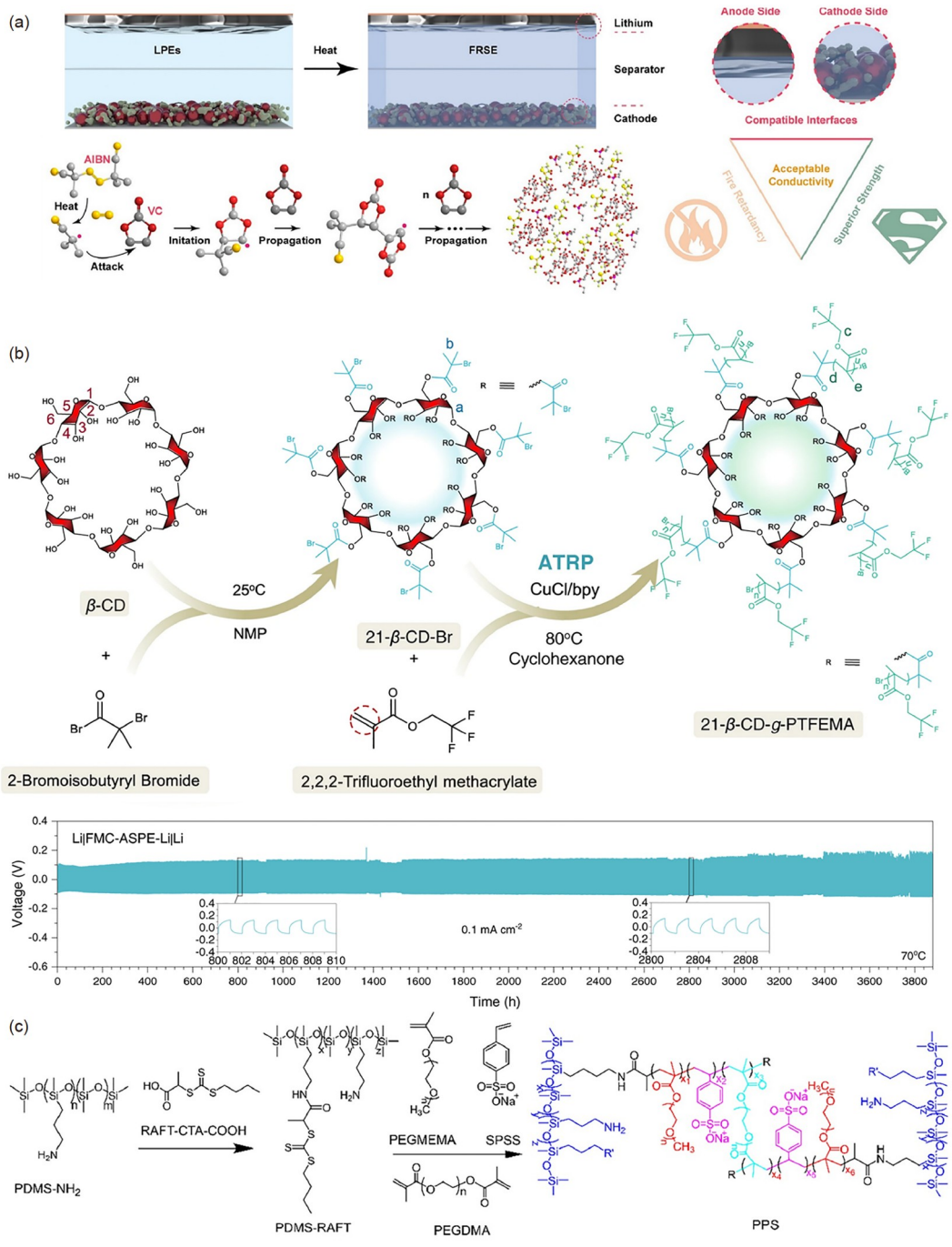

Figure 3 The reaction mechanisms of (a) uncontrolled free radical polymerization. Reproduced with permission Ref. [159]. Copyright 2021, Elsevier B. V. (b, c) Controlled free radical polymerization. (b) ATRP reaction. Reproduced with permission Ref. [166]. Copyright 2022, Nature Publication Group. (c) RAFT reaction. Reproduced with permission Ref. [168]. Copyright 2023, Elsevier B. V. (color online).

radical polymerization, Amici *et al*. [156] achieved a higher ionic conductivity by introducing large amount of ZrO_2 nanoparticles. Meanwhile, to achieve a high Li^+ transference number, single-ion conducting polymer electrolytes (SIPEs) has been developed, which can alleviate concentration polarization and achieve a uniform Li deposition. In 2013, Bouchet *et al*. [163] finely designed a BAB triblock single-ion polymer electrolyte, where the A block is based on a linear poly(ethylene oxide) (PEO) and the B block is based on poly(styrene trifluoromethanesulphonylimide of lithium) P(STFSILi), to achieve excellent mechanical properties and ionic conductivity (0.013 mS cm^{-1} at 60 °C) simultaneously. Combining the single-ion polymer electrolyte with the *in-situ* solidification techniques can further solve the problem of electrolyte/electrode interfacial resistance during the battery processing and manufacturing. Porcarelli *et al*. [164]

reported the novel SIPEs by the radical copolymerization of lithium 1-[3-(methacryloyloxy)propylsulfonyl]-1-(trifluoromethylsulfonyl)imide (LiMTFSI), poly(ethylene glycol) methyl ether methacrylate (PEGM) and bifunctional poly (ethylene glycol) methyl ether dimethacrylate (PEGDM). Under the *in-situ* solidification by synthesizing the SIPEs on the surface of LFP electrode, the assembled Li||SIPEs||LFP cells exhibited the capacity of 143 mAh g^{-1} at 1.0 C at 70 °C, and at higher current rates, it still maintains a high capacity. Furthermore, Zhang *et al*. [165] developed 3D cross-linked SIPEs by the *in-situ* thermally-initiated solidification of a novel Al-based lithium salt (perfluoropinacolatoaluminate (LiFPA). They simultaneously achieved a high-capacity retention (95.4% after 60 cycles) and improved thermal stability (onset temperature for heat release and thermal runaway temperature of 120 and 185 °C) with NCM811 cathodes in pouch cells, exhibiting more potential application for *in-situ* solidification electrolytes.

Although the reaction conditions of UFR polymerization are mild and easy to operate, its drawbacks are that it is not possible to realize the controllable and precise design of the polymerized electrolyte structure, which easily leads to the degradation of electrochemical performance.

3.1.2 Controlled free radical polymerization

By contrast, the controllable design of the structure and composition of polymerized electrolytes is of great importance and is expected to highlight the advantages of their high interfacial compatibility [23,132]. Generally, atom transfer radical polymerization (ATRP) combines the characteristics of radical polymerization and reactive polymerization. As a novel and precise polymerization reaction, ATRP enables controlled/active polymerization and the products can reach the desired molecular weight with a narrow molecular weight distribution. By taking these advantages, a lot of alkene monomers have been successfully synthesized with ATRP to produce structurally defined homopolymers, random copolymers, alternating copolymers, ladder copolymers, block/graft copolymers, and dendritic polymers as well as organic/inorganic hybrid materials. In addition, reversible addition-fracture chain transfer polymerization (RAFT) also possesses the chemical characteristics of a free radical reaction. At the initiation stage, free radicals must be introduced to produce monomer radicals and for the chain transfer and growth. In addition to common monomers, protonaceous monomers such as acrylic acid, aminomethyl methacrylate, or acid/basic monomers can be successfully polymerized. In view of this, CFR polymerization can be realized by ATRP and RAFT reactions, which are applicable to a wide range of monomers and are effective strategies for the design of macromolecules. In 2022, Su *et al*. [166] successfully designed a structurally well-defined "dobby" fluoropolymer combining poly(2,2,2-trifluoroethyl methacrylate) and poly(vinyl oxide) *via* the ATRP reaction, which could significantly broaden the electrochemical window and enhance the Li^+ transference number. Based on this, it can show a long cycle stability performance of nearly 4,000 h in Li||FMC-ASPE-Li||Li symmetric batteries at 70 °C (Figure 3b). Finally, the assembled Li||$LiMn_{0.6}Fe_{0.4}PO_4$ pouch cell can be stably cycled at the current density of 42 mA g^{-1} for 200 cycles under 70 °C and applied pressure of 0.28 MPa. Xie *et al*. [167] reported a four-armed polymers by the ATRP of the ether linkage from poly(ethyleneglycol) monomethacrylate–OH and poly(ethylene glycol) monomethacrylate–CH_3 to achieve the high ionic conductivity (0.49 mS cm^{-1}) and high Li^+ transfer number (0.46). Beyond that, the CFR polymerization can be achieved by the reversible addition-fracture transfer (RAFT) reaction. Gao *et al*. [168] prepared poly (dimethylsiloxane)-*g*-[poly(ethylene glycol) methyl ether methacrylate)-*r*-poly(sodium *p*-styrenesulfonate)] (PPS) multigraft polymer networks *via* the RAFT reaction. PPS has dual functions as an artificial SEI and a flexible solid-state electrolyte, and LMBs (Li||SPE||NMC811, Li||SPE||$LiFePO_4$) assembled based on PPS exhibit excellent cycling stability and safety (Figure 3c). Furthermore, Guo *et al*. [169] prepared block copolymer electrolytes (BCPEs) by using RAFT reaction and carboxylic acid-catalyzed ring-opening polymerization (ROP) in a one-step *in-situ* method. The Li^+ coordination can be systematically regulated by the BCPE, enabling fast Li^+ transfer between the anode and cathode in the LMBs. Then, the Li||BCPEs||LFP batteries deliver a high capacity-retention of up to 92% after 400 cycles at 1.0 C. Hu *et al*. [170] employed the RAFT reaction to prepare a copolymerized and crosslinked network-structured polymer (PEGMA-PEGDA), which exhibited excellent mechanical flexibility compared with the polymer produced by the UFR polymerization, and the combination with modified nanoparticles could greatly enhance the ionic conductivity of the polymerized electrolyte at room temperature.

3.2 Ionic polymerization

Ionic polymerization is also a common method to construct polymer electrolytes, which is an addition polymerization reaction, and generally divided into cationic polymerization and anionic polymerization [23,132].

3.2.1 Cationic polymerization

Cationic polymerization mainly adopts electrophilic reagents such as the protonate and Lewis acid (BF_3, BF_5, $B(C_6F_5)_3$, AlF_3, $Al(OTf)_3$, *etc*.) as initiators, which can be reacted under the conditions of room temperature, heating, high-energy radiation, *etc*. Correspondingly, the degree of the reaction depends on the activity strength of the initiator and mono-

mers, and common monomers are dominated by cyclic ethers and cyclic lactones. Moreover, it is worth noting that if the cationic reactivity is very high, it is very easy to induce various side reactions, so it is necessary to control the amount of initiator added to induce polymerization. Hwang *et al*. [171] adopted triethylene glycol divinyl ether (TEGDVE) as the monomer and added Lewis acid or protonate as the initiator for cationic polymerization to produce polymerized electrolytes with a wide electrochemical window (0–5 V) and high ionic conductivity (1.0 mS cm^{-1}), which displayed superior electrochemical performance when applied in batteries (Figure 4a). Moreover, the cationic ring-opening polymerization reaction is often dominated by the lone pair of electrons of the O atom in the cyclic ether monomers, which is easy to interact with the Lewis active site. Representatively, in 2019, Zhao *et al*. [152] introduced an aluminum salt of trifluoromethanesulfonate ($Al(OTf)_3$) as an initiator to trigger an *in-situ* ring-opening polymerization reaction of liquid DOL inside the battery to generate pDOLs with excellent mechanical/chemical stability, which achieves a high room-temperature ionic conductivity (>1 mS cm^{-1}) and low interfacial impedance. Notably, the pDOL can be successfully applied to LMBs with various cathode compositions (Li||S, Li||$LiFePO_4$, Li||$LiNi_{0.6}Mn_{0.2}Co_{0.2}O_2$), exhibiting excellent electrochemical performance (Figure 4b). More significantly, the above results of Zhao's research show that the strategy of "*in-situ* solidified polymer electrolytes" in batteries is very promising for a wider range of solid-state battery applications, and has successfully triggered a wave of research on ether-linked (–O–CH_2–CH_2–O–) polymer electrolytes. In 2019, Nair *et al*. [172] synthesized crosslinked polyether chain segment polymer electrolytes by using lithium salts as initiators in a cationic ring-opening polymerization reaction under heated conditions, which have a low glass-transition temperature (<−50 °C), high ionic conductivity (>0.1 mS cm^{-1}), and impressive oxidation re-

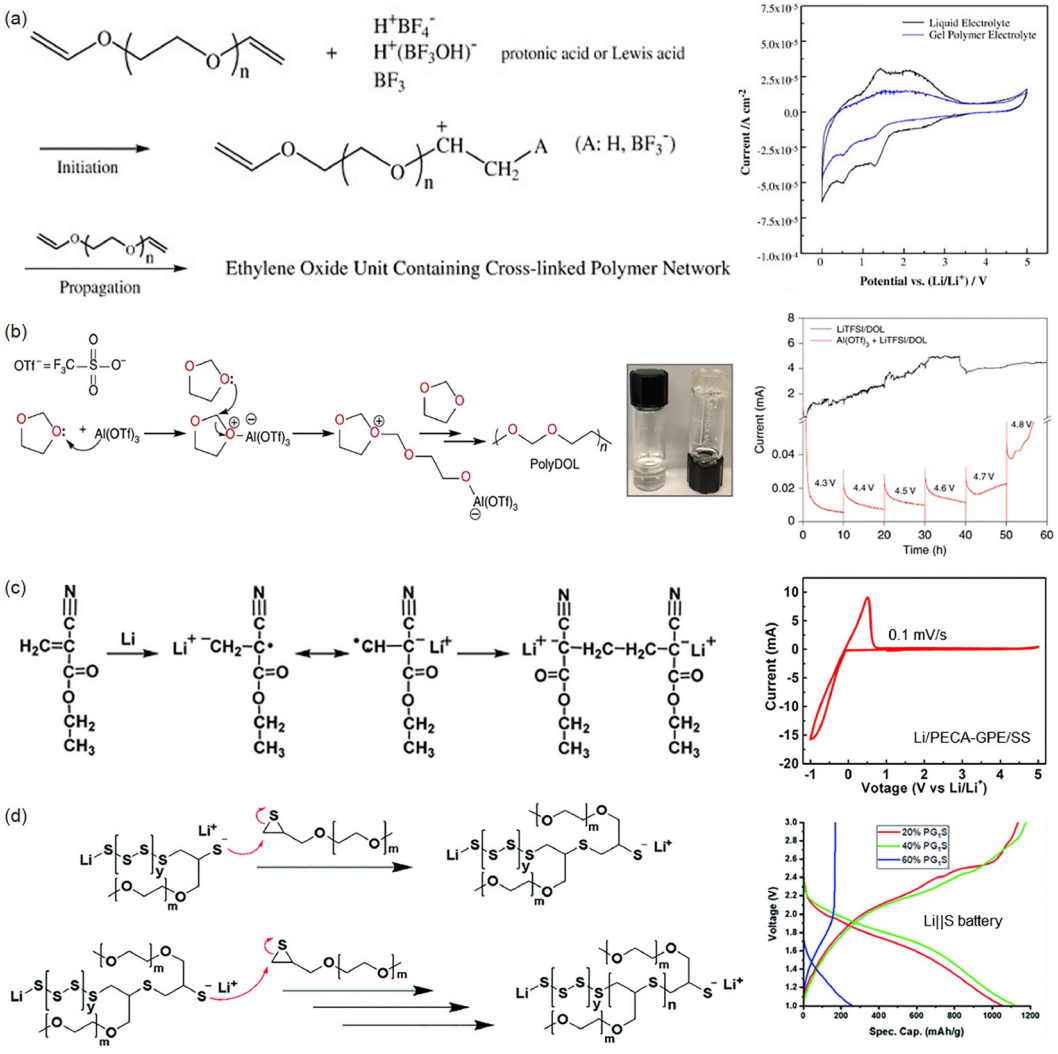

Figure 4 The reaction mechanisms of (a, b) cationic polymerization. Reproduced with permission Ref. [171]. Copyright 2010, Elsevier B. V. Reproduced with permission Ref. [152]. Copyright 2019, Nature publication group. (c, d) Anionic polymerization. Reproduced with permission Ref. [177]. Copyright 2017, American Chemical Society. Reproduced with permission Ref. [179]. Copyright 2021, the Royal Society of Chemistry (color online).

sistance at the high voltage (>5.5 V *vs*. Li^+/Li). In 2021, Chen *et al*. [173] designed a novel flexible and secure polymer electrolyte with 3D structure by combining *in-situ* polymerized pDOL with nanofiber membranes. In 2021, Xiang *et al*. [174] adopted *tris*(pentafluorophenyl)borane (TPFPB) as the initiator and flame-retardant to prepare DOL-based flame-retardant polymer electrolytes by *in-situ* solidification. Moreover, in 2022, Wen *et al*. [175] successfully prepared an ultrathin cross-linked solid polymer electrolyte (poly(DOL–TTE)–LP) by initiating simultaneous cationic ring-opening cross-coupling polymerization of trimethylolpropane triglycidyl ether (TTE) and DOL in an ultrathin porous polymer membrane *via* the *in-situ* solidification technique. To further enhance the mechanical properties of pDOL electrolytes, in 2023, Zhu *et al*. [176] developed for the first time a cationic ring-opening polymerization (CROP) *in-situ* cross-linking method using a four-armed cross-linking agent and prepared a cross-linked gel polymer electrolyte (c-GPE).

3.2.2 Anionic polymerization

Anionic polymerization mainly applies nucleophilic reagents such as organolithium compounds, metal alkanes, alkali metals, aminides and Grignard reagents as initiators. In view of the too active nucleophilic reagent, the reaction process needs to strictly control the reaction conditions to avoid the presence of water and oxygen, and is carried out in an inert atmosphere such as nitrogen, argon and other conditions. At the same time, the initiator itself is electron-rich, so that the polymerization monomers are mainly focused on unsaturated double-bonded olefinic monomers with electron-withdrawing substituents. In principle, once the anionic polymerization reaction has taken place, it is difficult to stop it until all monomers have been polymerized. Cui *et al*. [177] prepared PECA polymer electrolytes by anionic *in-situ* solidification based on the interaction of lithium metal anodes with ethyl cyanoacrylate (ECA) to generate an anionic initiator in a carbonate solvent of 4 mol L^{-1} $LiClO_4$, which showed an ionic conductivity as high as 2.7 mS cm^{-1} and a high-voltage resistance of 4.8 V. The assembled polymer LMBs with $LiFePO_4$ and $LiNi_{1.5}Mn_{0.5}O_4$ cathodes exhibit outstanding rate and long-cycle performance (Figure 4c). Zhou *et al*. [178] added lithium iodide (LiI) to vinylidene carbonate (VC) solvent, in which the I^- anion acted as an initiator to induce the solidification of VC to form PVC polymer electrolytes. In most cases, the ring-opening polymerization reactions of DOL are cationic polymerization reactions. Meisner *et al*. [179] discovered a new ring-opening polymerization mechanism of DOL in lithium–sulfur batteries, using cyclic sulfide as an initiator to carry out *in-situ* anionic ring-opening polymerization reactions (Figure 4d), which provides a new avenue of the exploration for the synthesis of polymer electrolytes.

3.3 Other polymerization

The polymer synthesis methods described above all require the introduction of an additional initiator to initiate the polymerization, which undoubtedly increases the cost and even introduces impurities. To deal with the aforementioned issue, polymer electrolytes can also be constructed by gamma-ray, electrochemical polymerization and gelation polymerization without the addition of an initiator [23,132]. For this, Park *et al*. [180] employed 10 MeV electron beam irradiation in a fully-assembled metal-shelled LIB to produce crosslinked poly(vinyl carbonate-*co*-cyanoacrylic acid ethyl ester) polymer electrolytes by the *in-situ* solidification in a short period of time (56 s) without adding any initiator or heat treatment (Figure 5a). Meanwhile, Wang *et al*. [181] adopted a one-step γ-radiation technique for the *in-situ* solidification of 3-(dimethylamino)propyl methacrylate and poly(ethylene glycol) diacrylate to produce polymer electrolytes with good thermal and mechanical stability. As we all know, the poor oxidation resistance of PEO-based polymer electrolytes makes it hard to match high-voltage cathode materials such as NCM811. Li *et al*. [182] employed an *in-situ* electropolymerization reaction strategy to construct a high-voltage-resistant poly(alkyl fluoroacrylate) interface layer on the surface of $LiNi_{0.8}Mn_{0.1}Co_{0.1}O_2$ (NCM811) cathode, which in turn improved the high-voltage stability of the PEO-based electrolytes from 4.3 to 5.1 V (Figure 5b), and still maintained the outstanding ionic conductivity (1.02×10^{-1} mS cm^{-1} at ambient temperature). Zhang *et al*. [183] employed acrylonitrile (AN) as an additive to form polyacrylonitrile (PAN) by the *in-situ* electrochemical polymerization on the surface of lithium metal anodes, which possesses excellent lithium-ion conductivity, improves lithium deposition behavior, and inhibits dendrite growth. Furthermore, Lei *et al*. [184] utilized the reaction between ethylenediamine and metallic lithium to generate lithium ethylenediamine as a gel factor, which triggered ethylene glycol dimethyl ether to carry out the *in-situ* crosslinking gel polymerization reaction. This gel can effectively alleviate the corrosion of the lithium metal anodes, so the lithium–air battery can be stably cycled for 1,175 h under high humidity conditions (Figure 5c). In view of this, the reaction diversity of *in-situ* solidified polymer systems depends on different solidification reaction mechanisms.

4 Applications of *in-situ* solidification in Li metal batteries

The application of polymer solid-state electrolytes to replace the flammable liquid electrolyte is a prominent step to promote the commercialization of LMBs. Meanwhile, in order to construct a high-energy-density battery system, it is often

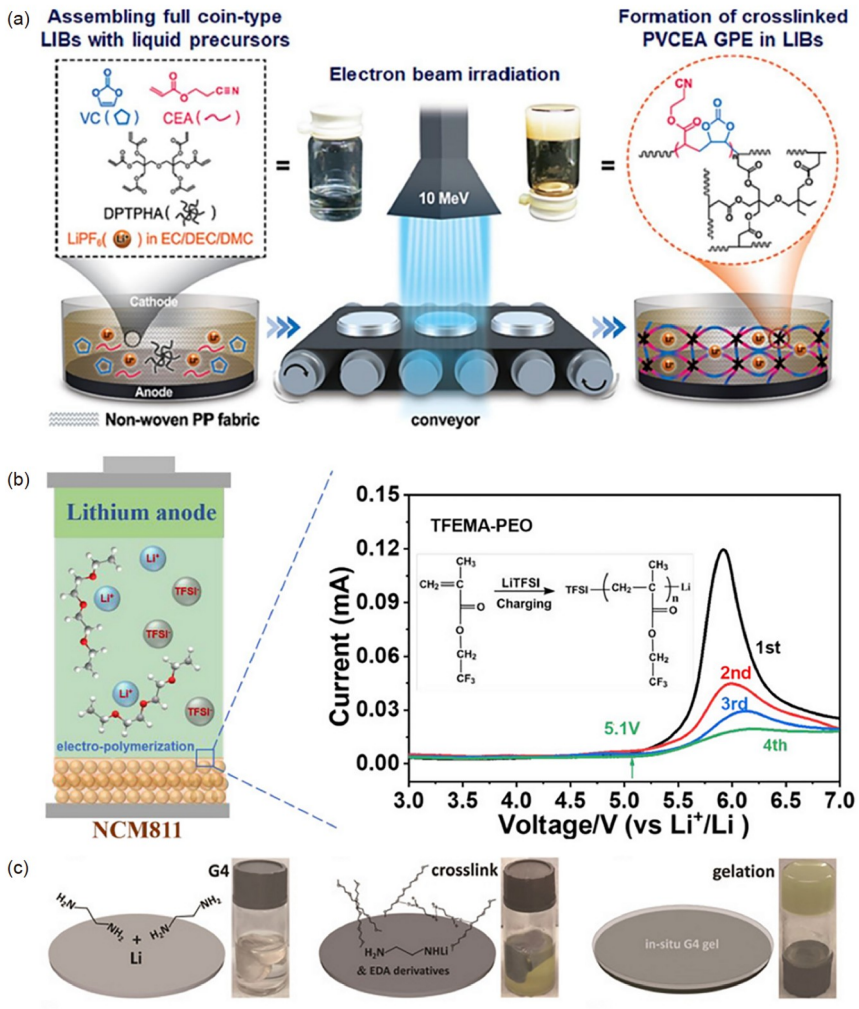

Figure 5 Other reaction mechanisms of (a) UV polymerization. Reproduced with permission Ref. [180]. Copyright 2023, Elsevier B. V; (b) electrochemical polymerization. Reproduced with permission Ref. [182]. Copyright 2022, American Chemical Society; (c) gel factor polymerization. Reproduced with permission Ref. [184]. Copyright 2018, Wiley-VCH (color online).

necessary to enhance the areal loading of active cathodes, resulting in an increase in the number of active particles. Regrettably, the contact between particles deteriorates, and the limited ion/electron transport contact points alone lead to increased polarization, retarded electrode process kinetics, and the difficulty in effectively exploiting the potential of high specific energy. In addition, the dendrite growth and "dead lithium" accumulation on the side of Li anodes under the high areal capacity, resulting in the dramatic loss of active Li and even short-circuit failure of the battery. Thereby, it can be seen that the poor solid–solid interface contact and dendrite growth is the fundamental origin to obstruct the application of solid-state LMBs. Based on the previous discussion and analysis of *in-situ* solidification, with the help of *in-situ* solidification technique to prepare *in-situ* solidified electrolytes to construct an excellent contact interface between the solid-state electrolytes and electrode materials to reduce the interface polarization. Furthermore, at the same time, it can also play a unique role in creating artificial interphase on the electrode surface.

4.1 Polymer electrolytes

Compared with the laboratory-grade coin-cell, the construction of practical pouch-cell systems faces greater challenges, such as higher active material loading and pouch-cell encapsulation. Therefore, it is important to address these challenges simultaneously. Notably, the adoption of the *in-situ* solidification method is compatible with the current production line of LIBs and easy to be scaled up. Accordingly, the solid-state LMBs employing *in-situ* solidified electrolytes are expected to better solve the above problems. In particular, they significantly improve the solid–solid interface contact between solid-state electrolyte/electrode material and electrode material/electrode material by injecting a liquid electrolyte to fill the entire electrode in the

pouch-cell system. Ultimately, the safety of the battery is further realized by the *in-situ* solidification. Based on the application of *in-situ* solidified electrolytes, they can be mainly categorized into integrated polymer electrolytes and asymmetric polymer electrolytes according to different preparation processes.

4.1.1 Integrated polymer electrolytes

Integrated polymer electrolytes mainly refer to polymer electrolytes that can be prepared by employing a one-step *in-situ* method without the need for step-by-step design of the polymer electrolyte structure in the battery [185–187]. Generally, before the polymerization, the suitable plasticizers or functional additives are often added to the precursor electrolyte to enhance the ionic conductivity and high voltage resistance of the polymer electrolyte system, so as to better accomplish the demands of the battery system. In 2018, Liu *et al*. [151] firstly reported the cationic ring-opening polymerization of DOL with the commercial lithium hexafluorophosphate ($LiPF_6$) under ambient conditions. To test the commercialization prospects, the GPE have been paired with many cathode materials. The Li||GPE||$LiFePO_4$ cells, with a bandgap of only 0.14 V in first 10 cycles, delivered an extremely high-capacity retention of 95.6% after 700 cycles. When paired with NCM622 with a voltage limitation of 4.3 V, GPE exhibited no obvious overcharging phenomenon, broadening the electrochemical window and breaking the limitation for liquid electrolytes under the high voltages. To improve the performance of pDOL electrolytes, Utomo *et al*. [188] introduced nano-sized SiO_2 particles (densely grafted with PEG chains) to develop hybrid solid-state polymer electrolytes (HSPEs), which can show high ionic conductivity at 25 °C (1.5 mS cm^{-1}) because the crystallization of pDOL is remarkably hindered by the PEG–SiO_2 structures. In LFP||GPE||Li cells, they can deliver high discharge capacity and stable plateau (Figure 6a). Zhao *et al*. [189] reported a dual functional additive of AlF_3 to achieve better performance of pDOL with high-voltage cathodes. On the one hand, AlF_3 can induce the cationic *in-situ* solidification of DOL. On the other hand, the introduction of AlF_3 in pDOL electrolytes creates a saturated Al^{3+} solution and immobilized $TFSI^-$ to inhibit the dissolution of Al_2O_3. Also, due to the contribution of AlF_3 to generate LiF in the CEI layer, the AlF_3-pDOL paired with NCM622 can show stable cycling performance at the cut-off voltage of 4.2 V (Figure 6b). Geng *et al*. [190] discovered the similar protection of the Al current collector from the corrosion in the presence of small amounts of $LiPF_6$. With the cooperative effect of FEC and HDI, the *in-situ* solidification electrolyte (poly-DOL-40FEC-HDI) can exhibit good cycling stability when paired with $LiCoO_2$ at 4.2 V. Apart from aluminum salts, researchers have been exploring other initiators. Yang *et al*. [191] reported the polymerization of DOL by the well-defined nanoparticles yttria-stabilized zirconia (YSZ), which can enhance the ionic conductivity (0.28 mS cm^{-1}) at the same time. When paired with NCM622 cathode, it can exhibit a long cycle lifetime of 800 cycles. Zheng *et al*. [192] reported the key role of tin trifluoromethanesulfonate ($Sn(OTf)_2$) in the DOL-based electrolyte. It can induce the *in-situ* solidification of DOL to achieve a semi-solid-state pDOL with a high ionic conductivity of 6.16×10^{-2} mS cm^{-1}. At the same time, Li–Sn alloy particles, reduced from the tin ions on the surface of lithium anodes, are benefit for the rapid charge transfer. Furthermore, Wang *et al*. [193] reported a novel *in-situ* cross-linked plastic crystal-based solidified electrolyte (CPCE), which delivers a broad electrochemical window and stable electrode/electrolyte interface. To be more specific, PCE was composed of dual lithium salt (LiTFSI, LiDFOB), while succinonitrile (SN) served as an efficient ion transport medium. After compounding with PCE, the monomer of ethoxylated trimethylolpropane triacrylate (ETPTA), which contains three carboxyl groups to effectively interact with SN, was *in-situ* crosslinking-solidified. The CPCE can exhibit an excellent ionic conductivity (1.08 mS cm^{-1}) at room temperature, high Li^+ transference number (0.54), and wide electrochemical stability window (5.4 V *vs*. Li^+/Li). When matched with a high-loading NCM622 cathode (~21.6 mg cm^{-2}), it maintains about 88.6% of the initial capacity after 40 cycles at 0.2 C. Recently, in order to apply the *in-situ* solidified electrolytes in the practical pouch cell, Chen *et al*. [194] performed the *in-situ* solidification technique to fabricate an ultra-thin SPE (8 μm) with extremely high ionic conductivity (3.3×10^{-2} mS cm^{-1}). For the *in-situ* solidified polymer skeleton, the carbonate esters group-riched monomer of the vinyl ethylene carbonate served as the conductive framework because its high dielectric constant and poly(ethylene glycol) diacrylate (PEGDA) served as the crosslinker to facilitate the mechanical strength. To test the capacity of polymer electrolytes to achieve high-energy-density, a 24 V bipolar pouch cell was assembled by a direct internal connection to light up a light-emitting diode (LED) (Figure 6c). Wu *et al*. [195] combined the ionic polymerization and free radical polymerization to develop a dual polymer network to enhance the electrolyte homogeneity. The DOL monomers were first induced by $Al(OTf)_3$ to polymerize and form the long chain skeleton, and then VC monomers were induced by AIBN under heating at 60 °C. The polymer electrolytes can exhibit both the good ionic conductivity (1.98 mS cm^{-1}), and a wide electrochemical stability window up to 4.3 V. Li||GPE||LFP cells can possess an initial discharge capacity of 117 mAh g^{-1} at 2 C with a high-capacity retention of 92.1% after 1,500 cycles.

4.1.2 Asymmetric polymer electrolytes

Asymmetric polymer electrolytes mainly refer to polymer

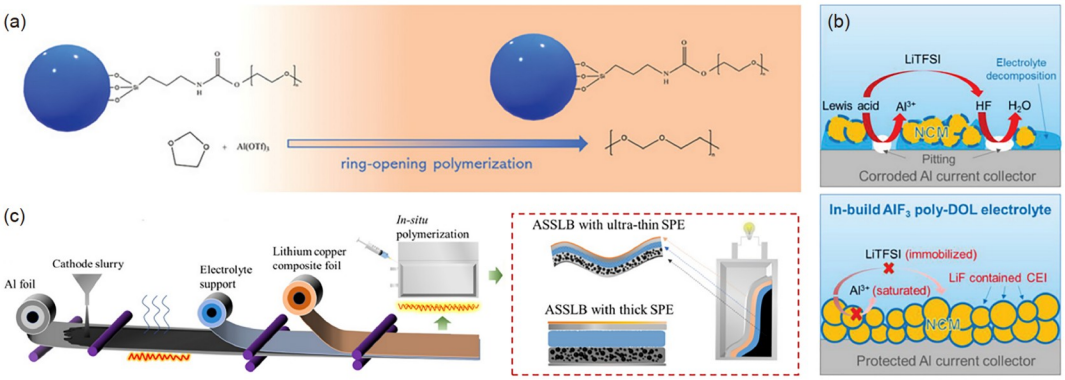

Figure 6 Integrated polymer electrolyte. (a) Schematic of *in situ* polymerization of DOL in the presence of HNPs. Reproduced with permission Ref. [188]. Copyright 2022, Wiley-VCH. (b) Schematic diagrams of current collector corrosion in routine electrolytes and AlF_3-pDOL electrolytes. Reproduced with permission Ref. [189]. Copyright 2020, Wiley-VCH. (c) Schematics of the preparation process for large scale production of ASSLB. Reproduced with permission Ref. [194]. Copyright 2022, Electrochemical Society, Inc. (color online).

electrolytes prepared by the two- or multi-step *in-situ* design. This asymmetric design tends to maximize the advantages of different types of polymer electrolytes. For example, PEO-based polymer electrolytes have high ionic conductivity and better compatibility with the lithium anode, but poor oxidation resistance. Alternatively, the modified carbonate-based polymer electrolytes have high oxidation resistance and better compatibility with the cathode, but low ionic conductivity. To this end, different polymer electrolytes are adopted to be pre-*in-situ* solidified on the side of anodes/cathodes, and fillers such as inorganic solid electrolytes can be compounded to synergize their advantages. Duan *et al.* [196] designed an asymmetric solid-state electrolyte (ASE), which performs high modulus to suppress the growth of dendrites on the anode and great flexibility to enhance the interface connection with active materials in the cathode, respectively. They coated LLZO nano-particles on the one side of the separators towards the Li metal anode. After assembling the batteries in order of the cathode, precursor solution, LLZO-coated separator and Li-metal, *in-situ* solidification was performed with the monomers poly(ethylene glycol) methyl ether acrylate (PEGMEA), which exhibits the low glass-transition temperature and wide electrochemical window. For symmetric Li||Li batteries with ASE, they exhibit stable lithium plating/stripping reversibility during cycling for 3,200 h with a stable voltage plateau (Figure 7a). To further enhance the stability of solid-state electrolytes when matched with high-voltage cathodes, Duan *et al.* [197] combined the *in-situ* solidification technique with the composite solid electrolytes and proposed a novel design of heterogeneous multilayered solid electrolyte (HMSE). The oxidation-tolerant poly(acrylonitrile) (PAN) polymer and PAN@LAGP electrolyte was chosen for the high-voltage cathodes, while the *in-situ* solidification of polyethylene glycol was performed on the surface of lithium anodes. The HMSE exhibits a wide electrochemical stability window of 0–5 V. When assembling LMBs with NCM811 cathodes, HMSE can show an excellent performance from 2.8 to 4.3 V and deliver a capacity of 175 mA h g^{-1} at 0.5 C with the negligible increased polarization during long-term cycling (Figure 7b). Furthermore, *in-situ* solidification was also reported to achieve bidirectionally functional polymer electrolytes (BDFPE) by Ma *et al.* [198]. The precursor monomer of pentaerythritol tetraacrylate (PETEA) was polymerized by UV light solidification, introducing nano-filler SiO_2 and TEP to match with the Ni-rich cathode. As for the lithium anode, PEO and FEC were added in another carbonate-based precursor of trimethylolpropane ethoxylate triacrylate (TPET), followed by the *in-situ* solidification. Due to the high ionic conductivity (5.84×10^{-1} mS cm^{-1}) and high Li^+ transference number (0.69) by BDFPE, a fast Li^+-flux is constructed to achieve stable lithium plating and striping at 1 mA cm^{-2} in symmetric Li||Li batteries for 1,800 h. When paired with NCM622, the *in-situ* solidified BDFPE can exhibit the lower transfer resistance and remarkable rate performance (Figure 7c). For traditional PEO-based electrolytes, Lu *et al.* [199] developed an *in-situ* cathode electrolyte interface (CEI)-coating method to enhance the stability under the high-voltage. After heating the precursor solution, vinylene carbonate (VC) was *in-situ* solidified. Also, a thin and uniform CEI layer on $LiCoO_2$ with the low resistance can be achieved by the addition of lithium difluoro(oxalato)borate. In the voltage range of 3.0–4.2 V, the coating strategy makes the cell deliver a high-capacity retention of 71.5% (101.6 mAh g^{-1}) after 500 cycles. (Figure 7d).

4.2 Artificial interphase

As the interface layer between electrode and electrolyte, the stable construction of artificial interphase is an important guarantee for achieving the excellent performance of LMBs.

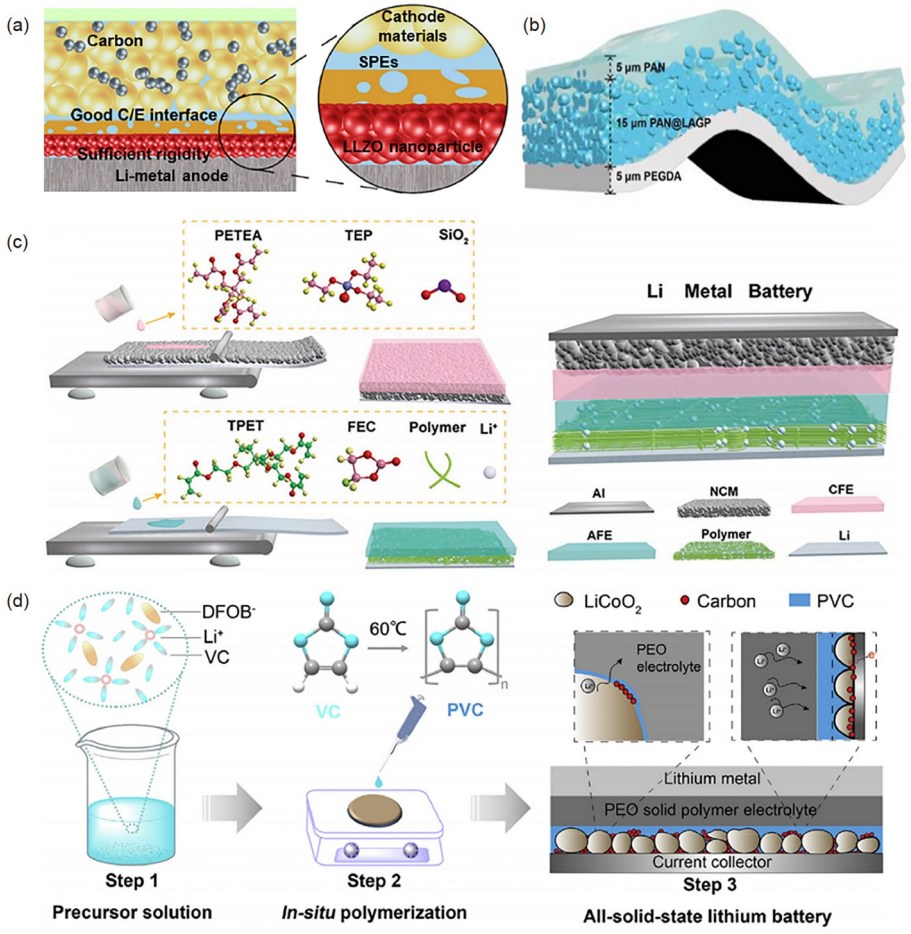

Figure 7 Asymmetric polymer electrolyte. (a) Schematic diagrams of solid Li metal batteries with SPEs. Reproduced with permission Ref. [196]. Copyright 2018, American Chemical Society. (b) Schematic diagram of the HMSE. Reproduced with permission Ref. [197]. Copyright 2019, Wiley-VCH. (c) Schematic diagram of preparation process for CFPE and AFPE. Reproduced with permission Ref. [198]. Copyright 2023, Wiley-VCH. (d) Schematic illustration of *in-situ* CEI coating and subsequent ASSLB assembly processes. Reproduced with permission Ref. [199]. Copyright 2020, Elsevier B. V. (color online).

4.2.1 Artificial interphase of cathodes

On the side of cathodes, the construction of an artificial interphase with strong oxidation resistance not only stabilizes the structure of the cathode material, but also serves as the isolation layer between the cathode material and the electrolyte to prevent the occurrence of side reactions and further enhance the high-voltage stability of the electrolyte [200,201]. Ultimately, the matched high-voltage cathode fulfills the potential of high-specific-energy. Cao *et al*. [202] reported an organic/inorganic composite SEI by *in-situ* solidification of poly (ethylene glycol) diacrylate (PEGDA) and the additive of lithium difluoro(oxalato)borate (LiDFOB). The intimate contact between the Li anode and SEI and high Li^+ conductivity at the interface is achieved by the *in-situ* solidification. In Li||NCM811 full cells with the artificial SEI, they exhibit the capacity retention of 58.4% after 300 cycles. Meanwhile, in the control group with bare Li, the capacity retention is only 12.2%. In Li||Li symmetrical cells, a long stable cycle of 700 h has been realized with the artificial SEI (Figure 8a). For PEO-based polymer electrolytes, Qiu *et al*. [203] introduced a facile interfacial engineering by the *in-situ* solidification of a PAN-based coating layer. In Li|| NCM532 full cells, they demonstrate a superior capacity retention of 72.3% after 200 cycles within 3.0–4.2 V. For lithium–sulfur (Li–S) batteries, in order to address the polysulfide dissolution and shuttle issues, Chen *et al*. [204] reported an *in-situ* solidification strategy triggered by 2,5-dichloro-1,4-benzoquinone (DCBQ) in the electrolyte. Polysulfides are covalently fixed by DCBQ in the form of solid organosulfur to enable effective immobilization of polysulfides.

4.2.2 Artificial interphase of lithium metal anodes

In addition, on the side of Li anodes, the introduction of a robust and flexible artificial interphase and the construction of organic/inorganic composite SEI can regulate the behavior of Li plating, inhibit the growth of dendrites, and significantly improve the reversibility of Li anodes [205]. Hu *et al*. [206] constructed a nitrogenous interface inorganic layer by *in-situ* solidification of ethyl α-cyanoacrylate pre-

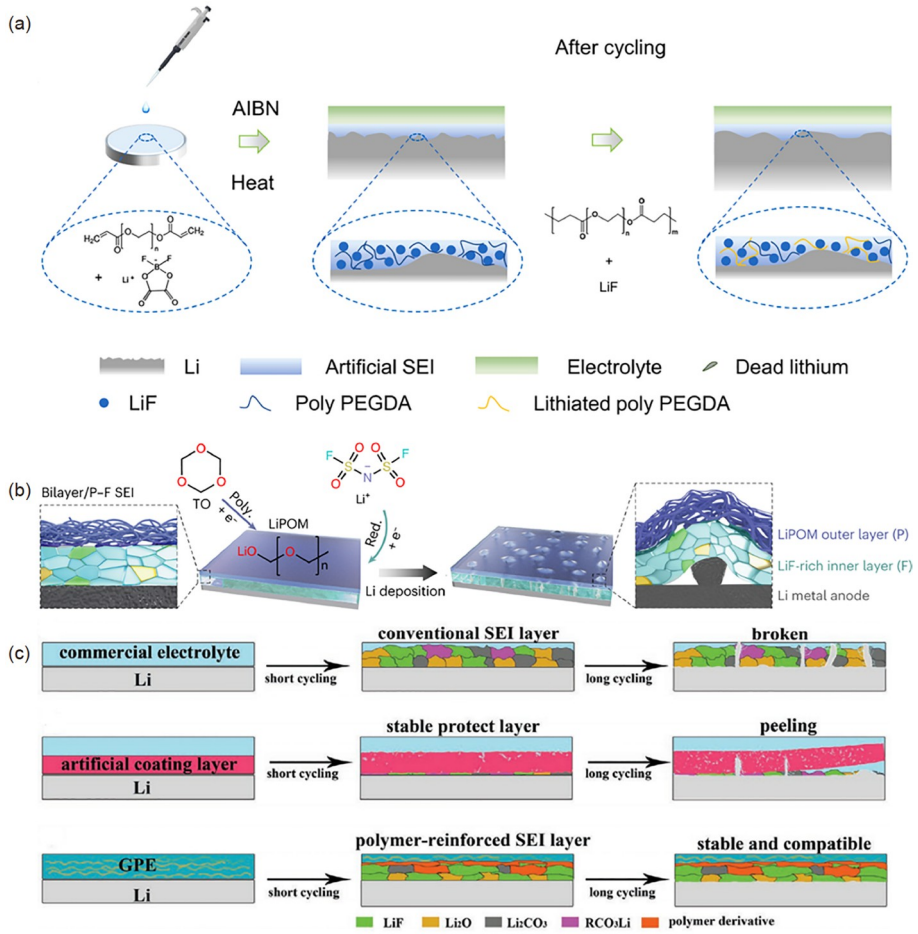

Figure 8 Artificial interphase. (a) Schematic illustration of organic/inorganic composite SEI preparation through *in-situ* solidification and the corresponding Li deposition behaviors of modified Li. Reproduced with permission Ref. [202]. Copyright 2022, Elsevier B. V. (b) Schematic diagram of the structural evolution of tailored bilayer SEIs during Li plating. Reproduced with permission Ref. [208]. Copyright 2023, Nature Publication Group. (c) Schematic diagram of the evolution of SEI layers during cycling within the batteries. Reproduced with permission Ref. [214]. Copyright 2020, Wiley-VCH (color online).

cursor with the $LiNO_3$ additive. For Li||LFP cells, they reach a capacity retention of 93% after 500 cycles at 2.0 C. To enhance cycling stability at high current densities, Wang *et al*. [207] developed a self-healable copolymer by *in-situ* RAFT polymerization of (PEO) segments and ureido-pyrimidinone (UPy) quadruple-hydrogen-bonding moieties. In symmetrical Li||Li cells, the LiPEO-UPy layer leads to a stable voltage profile during 2,000 h with only a low hysteresis of 45 mV at 5 mA cm^{-2} with 1 mAh cm^{-2}. By contrast, the bare Li||Li cells deliver short-circuits signals within 200 h. LiPEO-UPy||NCM full cells exhibit a high reversible capacity of 148.2 mAh g^{-1} at a rate of 1.0 C with a capacity retention of 84.2% after 200 cycles, enhancing the Li utilization by 14.8%. Moreover, Zhang *et al*. [208] designed a bilayer SEI: the inner layer mainly consists of inorganic LiF to achieve the homogenous Li^+-flux while the outer layer Li polyoxymethylene (LiPOM) was constructed by the *in-situ* solidification of trioxane (TO). For Li||Cu cells with bilayer SEI, Coulombic efficiency (CE) keeps as high as 99.5% within 400 cycles at a current density of 1.0 mA cm^{-2}. The bilayer SEI was further tested in Li||NCM523 full cells, which deliver a capacity retention over 80% during 430 cycles. Impressively, they successfully achieve a Li metal pouch-cell of 440 Wh kg^{-1} with a lifespan of 130 cycles (Figure 8b). Luo *et al*. [209] reported an organic film consisting of the anionic polymerization of Caffeic acid (CA), by introducing 1.0 wt% CA into the conventional electrolyte of 1.0 mol L^{-1} LiTFSI in the DOL/DME solution (*v*/*v*=1:1). The electrolyte is strongly interacted with the polymeric film by multiple hydrogen bonding, inhibiting the decomposition. The well-defined SEI, which is flexible and robust, successfully renders the uniform spherical Li deposition. Specifically, the *in-situ* RAFT polymerization has also been used to obtain a better SEI. Jin *et al*. [210] designed a polymer zwitterion-based artificial SEI layer with the sulfonate group and phosphate group to achieve stable cycles (1,400 h) in a full cell. Xiong *et al*. [211] constructed a conformal polyaniline (PANI) layer on the Cu substrate by the *in-situ* solidification and cyclic voltammetry (CV) method. The lithiophilic PANI layer can reduce the lithium nucleation/

plating overpotential to realize uniform and dense lithium deposition. As a result, lithium metal anodes modified with PANI show high Coulombic efficiency (CE) (99.1%) for 400 cycles. Furthermore, in PEO-based LMBs, to probe the formation mechanism of the electrode interface [212,213], Sheng *et al*. [213] introduced Li_2S additive to harvest stable all-solid-state LMBs, which verified the *in-situ* construction of a LiF-enriched interface *via* cryo-transmission electron microscopy (Cryo-TEM) results. For gel polymer electrolytes, Hu *et al*. [214] introduced cyclic carbonate urethane methacrylate for the *in-situ* solidification of a robust homopolymer as the SEI. A mechanically improved SEI layer can be realized by the anionic ring-opening polymerization of the cyclic carbonate. And the Li||$LiCoO_2$ full cells can show a capacity retention of 92% after 200 cycles at 0.5 C (Figure 8c). In summary, we made a summary of the application of *in-situ* solidification in Li metal batteries *via* adopting the *in-situ* solidification technology, which include the monomer, initiator, ionic conductivity, high-voltage resistance and electrochemical performance of polymer electrolytes, as shown in Table 1.

5 Summary and outlook

With the rapid popularization of new energy electric vehicles, the social demand for the high-specific-energy battery system is increasingly high, and LMBs are favored because of the high-energy-density potential of 500 Wh kg^{-1}. Regrettably, the conventional liquid LMBs are highly susceptible to fire or even explosion, thus it is necessary to explore high-safety solid-state LMBs, but there is an urgent need to solve the puzzle of poor solid–solid contact and dendritic lithium growth. Recent researches claimed that the *in-situ* solidification technology plays a significant role in enhancing the safety of LMBs, especially breaking through the inherent bottleneck of poor interfacial compatibility and dendrite growth in high areal capacity cycling conditions. This paper reviews the development of *in-situ* solidification technology, as well as the various synthesis methods for *in-situ* solidification, such as uncontrolled/controlled free radical polymerization, cationic/anionic polymerization, and other polymerization methods. Based on the knowledge and understanding of *in-situ* solidification, combined with the functionalization requirements of polymer electrolytes, integrated polymer electrolytes and asymmetric polymer electrolytes are designed and introduced into high-energy-density battery systems, which effectively improves the solid–solid interfacial compatibility between the electrolyte/electrode and electrode/electrode. At the same time, the construction of a stable and robust artificial interphase can regulate the composition of SEI/CEI in the field of molecular structure, thus inhibiting the growth of dendrites and improving the high-voltage stability of electrolytes and cathode materials.

The development of *in-situ* solidification technology is still in its infancy, with many opportunities and challenges in the process of designing next-generation batteries with high power, durability and safety.

(1) *In-situ* solidification strategies outside the battery have many limitations, and there is strong request to establish a link with *in-situ* solidification inside the battery to achieve superior solid–solid interfacial contact.

(2) In polymer LMBs, the high ionic conductivity and strong oxidation resistance of the polymer electrolyte are the key factors to exhibit excellent electrochemical performance. Consequently, it is necessary to explore the mechanism of various structures and groups in the polymer chains on the lithium-ion transport to realize the directional design of the monomer structure and polymer functionalization in the electrolyte.

(3) Explore the reaction/transport mechanism of lithium ions across the boundary between the solidified electrolyte and the anode/cathode interface, and further improve the electrochemical and thermal stability of the polymer electrolyte in order to extend their cycling lifetime.

(4) Different solidification methods are adopted to ensure that each electrode particle surface is uniformly film-forming and remains intact as the particle deforms. In addition, in order to demonstrate the role of plasticizers at different times, it is necessary to develop relevant techniques such as gel permeation chromatography (GPC), NMR and other tests to monitor the *in-situ* solidification process, quantification of solidification products and standardization of plasticizers.

(5) From the high-voltage cathode to the low-voltage Li anode, it is hard for a single polymer system to fulfill the requirements, so it is necessary to integrate the inorganic solid-state electrolyte and organic system to play a synergistic role. Such as the employment of suitable inorganic and organic substances to construct a robust interphase on the positive and negative electrode surface *via* the pre-coating/modification method, and then with the help of various polymer electrolytes to fill the gap of them, and to ensure that the preparation process of the components does not return to the mixure.

(6) Based on the understanding and design of multilayer polymer electrolytes, a continuous 3D porous skeleton is combined to achieve rapid Li^+ migration and highly reversible lithium plating/stripping performance.

(7) Develop single-ion polymer electrolytes and high-performance MOF/COF/POM/polymer composite electrolytes and functional additives.

(8) How the interfacial resistance between solid-state electrolytes is avoided and how well are ion channels matched? How the repair function of ion channels as the elec-

Table 1 The performance of *in-situ* solidification in Li metal batteries *via* adopting the *in-situ* solidification technology

	Monomer	Initiator	High-voltage resistance	Ionic conductivity	Electrochemical performance (LMB full cells)	Ref.
Integrated polymer electrolyte	DOL	2 mol L^{-1} $LiPF_6$	4.6 V (Li||SS 1.0 mV s^{-1})	3.8 mS cm^{-1} 25 °C	Li||GPE||$LiFePO_4$, 0.5 C (capacity retention of 95.6% after 700 cycles) Li||S, 0.5 C (capacity retention of 73.7% after 500 cycles)	[151]
	DOL	10 mmol L^{-1} $Al(OTf)_3$	4.75 V (Li||SS 1.0 mV s^{-1})	1.5 mS cm^{-1} 25 °C	Li||$LiFePO_4$, 0.2 C (capacity retention of 54.5% after 100 cycles) Li||sPAN, 0.1 C (capacity retention of 45.0% after 100 cycles)	[188]
	DOL	0.5 mmol L^{-1} $Al(OTf)_3$ 0.3 mol L^{-1} AlF_3	4.4 V (Li||Al 0.02 mV s^{-1})	mS cm^{-1} level 25 °C	Li||$LiNi_{0.6}Co_{0.2}Mn_{0.2}O_2$, 0.1 C (capacity retention of 80.6% after 50 cycles)	[189]
	DOL	0.2 mol L^{-1} LiDFOB 0.01 mol L^{-1} $LiPF_6$	4.6 V (Li||SS 0.1 mV s^{-1})	1.0 mS cm^{-1} 25 °C	Li||$LiCoO_2$, 0.5 C (capacity retention of 80.0% after 500 cycles)	[190]
	DOL	Yttria-stabilized zirconia	4.9 V (Li||SS 0.2 mV s^{-1})	0.275 mS cm^{-1} 20 °C	Li||$LiNi_{0.6}Co_{0.2}Mn_{0.2}O_2$, 0.5 C (capacity retention of 74% after 800 cycles)	[191]
	DOL	2.0 mmol L^{-1} $Sn(OTf)_2$	4.4 V	0.0616 mS cm^{-1} 25 °C 1.0 mS cm^{-1} 70 °C	Li||$LiFePO_4$, 0.5 C (capacity retention of 93.1% after 200 cycles) Li||$LiCoO_2$, 0.5 C (no obvious capacity fade after 100 cycles) Li||S, 0.2 C (capacity retention of 66.1% after 300 cycles)	[192]
	Ethoxylated trimethylolpropane triacrylate	0.5 wt.% AIBN	5.4 V (Li||SS 1.0 mV s^{-1})	1.08 mS cm^{-1} 40 °C	Li||CPCE||$LiCoO_2$, 0.5 C (capacity retention of 94.2% after 300 cycles)	[193]
	Poly(ethylene glycol) diacrylate	0.5 wt.% AIBN	4.5 V (Li||SS 1.0 mV s^{-1})	1.0 mS cm^{-1} 25 °C	Li||$LiFePO_4$, 0.2 C, 60 °C (capacity retention of 86.0% after 150 cycles)	[194]
	DOL+Vinylene carbonate	0.5 mmol L^{-1} $Al(CF_3SO_3)_3$ and 0.5 wt.% AIBN	4.3 V (Li||SS 0.1 mV s^{-1})	1.98 mS cm^{-1} 25 °C	Li||$LiFePO_4$, 2.0 C (capacity retention of 92.1% after 1,500 cycles)	[195]
Asymmetric polymer electrolyte	Poly(ethylene glycol) methyl ether acrylate	1.0 wt.% BPO	4.8 V (Li||SS 0.1 mV s^{-1})	0.1 mS cm^{-1} 40 °C	Li||$LiFePO_4$, 0.2 C, 55 °C (capacity retention of 94.5% after 120 cycles)	[196]
	Poly(acrylonitrile)+ Polyethylene glycol diacrylate	1.0 wt.% 2-hydroxy-2-methyl-1-phenyl-1-propanon	5.0 V (Li||SS 0.1 mV s^{-1})	0.37 mS cm^{-1} 25 °C	Li||$LiNi_{0.6}Co_{0.2}Mn_{0.2}O_2$, 0.5 C (capacity retention of 81.5% after 270 cycles)	[197]
	Trimethylolpropane ethoxylate triacrylate+ Pentaerythritol tetraacrylate	1.0 wt.% 2-hydroxy-2-methyl-1-phenyl-1-propanon	4.5 V (Li||SS 0.1 mV s^{-1})	0.584 mS cm^{-1} 25 °C	Li||$LiNi_{0.6}Co_{0.2}Mn_{0.2}O_2$, 5.0 C (capacity retention of 84.0% after 150 cycles)	[198]
	Vinylene carbonate (VC)	1 mg AIBN into 1 mL VC	5.0 V (Li||SS 1.0 mV s^{-1}, 60 °C)	0.263 mS cm^{-1} 60 °C	Li||$LiCoO_2$, 0.5 C (capacity retention of 71.5 % after 500 cycles)	[199]

trode material ages is realized?

(9) In a thermal runaway scenario, can the organic solid electrolyte act as a flame retardant substance and be able to enhance the safety of the battery?

(10) For precursor solutions with different viscosities and wettability, it is necessary to develop appropriate separators in terms of material selection, porosity optimization, inorganic coating technique, and thermal stability.

(11) SEI/CEI interphase in polymer-based lithium metal batteries should be studied with the help of advanced char-

acterization techniques such as cryo-transmission electron microscopy (Cryo-TEM). Meanwhile, the exploration of multifunctional solid-state electrolytes through machine learning is highly expected for matching relevant electrodes.

(12) For commercialized applications, especially for the large battery core, how to ensure uniformity, solidification, batch stability, and how to avoid thermal effects in solidification, are not only a matter of electrode/electrolyte designs to enhance the ionic conductivity, optimize the porous electrode structure, or improve the electrolyte stability, but also the structure involved and the injection method. In addition, the preparation process for *in-situ* solidification and its adaptability to different/extreme environmental conditions, *etc*., need to be considered.

(13) A green and optimized battery system facilitates the functioning of electrode materials in different cycles, and it is necessary to carry out core design and solid-state electrolyte recycling from the recycling point of view.

Collectively, to better solve and break through the above problems, it is necessary to combine the current advanced characterization techniques such as *in-situ* optical-pressure-coupling device, solid-state nuclear magnetic resonance (SSNMR), time-of-flight secondary ion mass spectrometry (TOF-SIMS) and cryo-electron microscopy (Cryo-EM), and with the help of new computational methods, such as machine learning, artificial intelligence development, the polymer electrolyte structure of the functionalization of the screening, design, and reveal the dynamic evolution of the interface of the solid-state batteries, and then construct the next-generation of high-energy-density, high-safety LMBs.

Acknowledgements This work was supported by Beijing Municipal Natural Science Foundation (Z200011), National Key Research and Development Program of China (2021YFB2500300, 2021YFB2400300), National Natural Science Foundation of China (22308190, 22109084, 22108151, 22075029, and 22061132002), Key Research and Development Program of Yunnan Province (202103AA080019), the S&T Program of Hebei Province (22344402D), China Postdoctoral Science Foundation (2022TQ0165), Tsinghua-Jiangyin Innovation Special Fund (TJISF), Tsinghua-Toyota Joint Research Fund and the Institute of Strategic Research, Huawei Technologies Co., Ltd, and Ordos-Tsinghua Innovative & Collaborative Research Program in Carbon Neutrality. P.X. appreciate the Shuimu Tsinghua Scholar Program of Tsinghua University.

Conflict of interest The authors declare no conflict of interest.

1 Liu J, Bao Z, Cui Y, Dufek EJ, Goodenough JB, Khalifah P, Li Q, Liaw BY, Liu P, Manthiram A, Meng YS, Subramanian VR, Toney MF, Viswanathan VV, Whittingham MS, Xiao J, Xu W, Yang J, Yang XQ, Zhang JG. *Nat Energy*, 2019, 4: 180–186
2 Larcher D, Tarascon JM. *Nat Chem*, 2014, 7: 19–29
3 Meng YS. *Chem Rev*, 2020, 120: 6327
4 Long W, Fang B, Ignaszak A, Wu Z, Wang YJ, Wilkinson D. *Chem Soc Rev*, 2017, 46: 7176–7190
5 Yao YX, Zhang XQ, Li BQ, Yan C, Chen PY, Huang JQ, Zhang Q. *InfoMat*, 2019, 2: 379–388
6 Feng S, Fu ZH, Chen X, Zhang Q. *InfoMat*, 2022, 4: e12304
7 Li XY, Zhang Q. *J Energy Chem*, 2022, 65: 302–303
8 Zhao CX, Chen WJ, Zhao M, Song YW, Liu JN, Li BQ, Yuan T, Chen CM, Zhang Q, Huang JQ. *EcoMat*, 2020, 3: e12066
9 Liang X, Wang L, Wu X, Feng X, Wu Q, Sun Y, Xiang H, Wang J. *J Energy Chem*, 2022, 73: 370–386
10 Liang Y, Zhao CZ, Yuan H, Chen Y, Zhang W, Huang JQ, Yu D, Liu Y, Titirici MM, Chueh YL, Yu H, Zhang Q. *InfoMat*, 2019, 1: 6–32
11 Kong L, Tang C, Peng HJ, Huang JQ, Zhang Q. *SmartMat*, 2020, 1: e1007
12 Yang Q, Jiang N, Shao Y, Zhang Y, Zhao X, Zeng Y, Qiu J. *Sci China Chem*, 2022, 65: 2351–2368
13 Luo B, Zhi L. *Energy Environ Sci*, 2015, 8: 456–477
14 Chang H, Wu H. *Energy Environ Sci*, 2013, 6: 3483
15 Chen K, Song S, Liu F, Xue D. *Chem Soc Rev*, 2015, 44: 6230–6257
16 Kumar R, Sahoo S, Joanni E, Singh RK, Tan WK, Kar KK, Matsuda A. *Prog Energy Combust Sci*, 2019, 75: 100786
17 Zhang QK, Zhang XQ, Yuan H, Huang JQ. *Small Sci*, 2021, 1: 2100058
18 Liu H, Cheng X, Chong Y, Yuan H, Huang JQ, Zhang Q. *Particuology*, 2021, 57: 56–71
19 Zhu X, Wang K, Xu Y, Zhang G, Li S, Li C, Zhang X, Sun X, Ge X, Ma Y. *Energy Storage Mater*, 2021, 36: 291–308
20 Tan SJ, Wang WP, Tian YF, Xin S, Guo YG. *Adv Funct Mater*, 2021, 31: 2105253
21 Tarascon JM, Armand M. *Nature*, 2001, 414: 359–367
22 Lin D, Liu Y, Cui Y. *Nat Nanotech*, 2017, 12: 194–206
23 Vijayakumar V, Anothumakkool B, Kurungot S, Winter M, Nair JR. *Energy Environ Sci*, 2021, 14: 2708–2788
24 Wan M, Kang S, Wang L, Lee HW, Zheng GW, Cui Y, Sun Y. *Nat Commun*, 2020, 11: 829
25 Xu P, Lin X, Hu X, Cui X, Fan X, Sun C, Xu X, Chang JK, Fan J, Yuan R, Mao B, Dong Q, Zheng M. *Energy Storage Mater*, 2020, 28: 188–195
26 Xu P, Hu X, Liu X, Lin X, Fan X, Cui X, Sun C, Wu Q, Lian X, Yuan R, Zheng M, Dong Q. *Energy Storage Mater*, 2021, 38: 190–199
27 Lee J, Choi JW. *EcoMat*, 2022, 4: e12193
28 Ran Q, Zhao H, Liu J, Li L, Hu Q, Nie F, Liu X, Kormarneni S. *J Energy Chem*, 2023, 82: 475–483
29 Jiang FN, Yang SJ, Chen ZX, Liu H, Yuan H, Liu L, Huang JQ, Cheng XB, Zhang Q. *Particuology*, 2023, 79: 10–17
30 Jiang LL, Yan C, Yao YX, Cai W, Huang JQ, Zhang Q. *Angew Chem Int Ed*, 2020, 60: 3402–3406
31 Han S, Li Z, Zhang Y, Lei D, Wang C. *Energy Storage Mater*, 2022, 48: 384–392
32 Huang J, Zhang H, Yuan X, Sha Y, Li J, Dong T, Song Y, Zhang S. *Chem Eng J*, 2023, 464: 142578
33 Zuo W, Luo M, Liu X, Wu J, Liu H, Li J, Winter M, Fu R, Yang W, Yang Y. *Energy Environ Sci*, 2020, 13: 4450–4497
34 Sun H, Zhu G, Zhu Y, Lin MC, Chen H, Li YY, Hung WH, Zhou B, Wang X, Bai Y, Gu M, Huang CL, Tai HC, Xu X, Angell M, Shyue JJ, Dai H. *Adv Mater*, 2020, 32: 2001741
35 Seo J, Im J, Yoon S, Cho KY. *Chem Eng J*, 2023, 470: 144406
36 Zhang JG, Xu W, Xiao J, Cao X, Liu J. *Chem Rev*, 2020, 120: 13312–13348
37 Lee Y, Lee TK, Kim S, Lee J, Ahn Y, Kim K, Ma H, Park G, Lee SM, Kwak SK, Choi NS. *Nano Energy*, 2020, 67: 104309
38 Wang Z, Sun Z, Li J, Shi Y, Sun C, An B, Cheng HM, Li F. *Chem Soc Rev*, 2021, 50: 3178–3210
39 Shen X, Zhang XQ, Ding F, Huang JQ, Xu R, Chen X, Yan C, Su FY, Chen CM, Liu X, Zhang Q. *Energy Mater Adv*, 2021, 2021: 1205324
40 Liu H, Cheng X, Yan C, Li Z, Zhao C, Xiang R, Yuan H, Huang J, Kuzmina E, Karaseva E, Kolosnitsyn V, Zhang Q. *iEnergy*, 2022, 1: 72–81
41 Yang Y, Yan C, Huang J. *Acta Physico Chim Sin*, 2020, 37: 2010076
42 Wu Y, Feng X, Liu X, Wang X, Ren D, Wang L, Yang M, Wang Y, Zhang W, Li Y, Zheng Y, Lu L, Han X, Xu GL, Ren Y, Chen Z,

Chen J, He X, Amine K, Ouyang M. *Energy Storage Mater*, 2021, 43: 248–257
43 Chen R, Li Q, Yu X, Chen L, Li H. *Chem Rev*, 2019, 120: 6820–6877
44 Xu XQ, Cheng XB, Jiang FN, Yang SJ, Ren D, Shi P, Hsu HJ, Yuan H, Huang JQ, Ouyang M, Zhang Q. *SusMat*, 2022, 2: 435–444
45 Xie H, Hao Q, Jin H, Xie S, Sun Z, Ye Y, Zhang C, Wang D, Ji H, Wan LJ. *Sci China Chem*, 2020, 63: 1306–1314
46 Qi S, Wang H, He J, Liu J, Cui C, Wu M, Li F, Feng Y, Ma J. *Sci Bull*, 2021, 66: 685–693
47 Jiang FN, Yang SJ, Liu H, Cheng XB, Liu L, Xiang R, Zhang Q, Kaskel S, Huang JQ. *SusMat*, 2021, 1: 506–536
48 Pei F, Lin L, Fu A, Mo S, Ou D, Fang X, Zheng N. *Joule*, 2018, 2: 323–336
49 Pei F, Lin L, Ou D, Zheng Z, Mo S, Fang X, Zheng N. *Nat Commun*, 2017, 8: 482
50 Pei F, Fu A, Ye W, Peng J, Fang X, Wang MS, Zheng N. *ACS Nano*, 2019, 13: 8337–8346
51 Li S, Xu P, Aslam MK, Chen C, Rashid A, Wang G, Zhang L, Mao B. *Energy Storage Mater*, 2020, 27: 51–60
52 Xu P, Yan MY, Yu SS, Liu XY, Fan JM, Yuan RM, Zheng MS, Dong QF. *Chem Eng J*, 2022, 431: 133906
53 Hu XY, Xu P, Deng S, Lei J, Lin X, Wu QH, Zheng M, Dong Q. *J Mater Chem A*, 2020, 8: 17056–17064
54 Li Y, Xu P, Chen G, Mou J, Xue S, Li K, Zheng F, Dong Q, Hu J, Yang C, Liu M. *Chem Eng J*, 2020, 380: 122595
55 Liu X, Xu P, Zhang J, Hu X, Hou Q, Lin X, Zheng M, Dong Q. *Small*, 2021, 17: 2102016
56 Liu J, Yuan H, Tao X, Liang Y, Yang SJ, Huang JQ, Yuan TQ, Titirici MM, Zhang Q. *EcoMat*, 2020, 2: e12019
57 Zhao M, Li XY, Chen X, Li BQ, Kaskel S, Zhang Q, Huang JQ. *eScience*, 2021, 1: 44–52
58 Wang Z, Du Z, Liu Y, Knapp CE, Dai Y, Li J, Zhang W, Chen R, Guo F, Zong W, Gao X, Zhu J, Wei C, He G. *eScience*, 2023, 100189
59 Paul-Orecchio AG, Stockton L, Weeks JA, Dolocan A, Wang Y, Mullins CB. *ACS Energy Lett*, 2023, 8: 4228–4234
60 Ye H, Lei D, Shen L, Ni B, Li B, Kang F, He YB. *Chin Chem Lett*, 2020, 31: 570–574
61 Liu T, Zhang J, Han W, Zhang J, Ding G, Dong S, Cui G. *J Electrochem Soc*, 2020, 167: 070527
62 Cheng XB, Zhang R, Zhao CZ, Zhang Q. *Chem Rev*, 2017, 117: 10403–10473
63 Ding P, Lin Z, Guo X, Wu L, Wang Y, Guo H, Li L, Yu H. *Mater Today*, 2021, 51: 449–474
64 Chai S, Zhang Y, Wang Y, He Q, Zhou S, Pan A. *eScience*, 2022, 2: 494–508
65 Hu JK, Yuan H, Yang SJ, Lu Y, Sun S, Liu J, Liao YL, Li S, Zhao CZ, Huang JQ. *J Energy Chem*, 2022, 71: 612–618
66 Sun S, Zhao CZ, Yuan H, Lu Y, Hu JK, Huang JQ, Zhang Q. *Mater Futures*, 2022, 1: 012101
67 Pei F, Dai S, Guo B, Xie H, Zhao C, Cui J, Fang X, Chen C, Zheng N. *Energy Environ Sci*, 2021, 14: 975–985
68 Liu J, Yuan H, Liu H, Zhao CZ, Lu Y, Cheng XB, Huang JQ, Zhang Q. *Adv Energy Mater*, 2021, 12: 2100748
69 Xu L, Li J, Shuai H, Luo Z, Wang B, Fang S, Zou G, Hou H, Peng H, Ji X. *J Energy Chem*, 2022, 67: 524–548
70 Yu W, Deng N, Tang L, Cheng K, Cheng B, Kang W. *Particuology*, 2022, 65: 51–71
71 Liang Y, Liu H, Wang G, Wang C, Ni Y, Nan CW, Fan LZ. *InfoMat*, 2022, 4: e12292
72 Liu Q, Chen Q, Tang Y, Cheng HM. *Electrochem Energy Rev*, 2023, 6: 15
73 Lu Y, Zhao CZ, Yuan H, Cheng XB, Huang JQ, Zhang Q. *Adv Funct Mater*, 2021, 31: 2009925
74 Zhu G, Zhao C, Yuan H, Nan H, Zhao B, Hou L, He C, Liu Q, Huang J. *Acta Physico Chim Sin*, 2021, 37: 2005003
75 Fu ZH, Chen X, Yao N, Shen X, Ma XX, Feng S, Wang S, Zhang R, Zhang L, Zhang Q. *J Energy Chem*, 2022, 70: 59–66
76 Chen H, Cao X, Huang M, Ren X, Zhao Y, Yu L, Liu Y, Zhong L, Qiu Y. *J Energy Chem*, 2023, DOI:10.1016/j.jechem.2023.09.020
77 Randau S, Weber DA, Kötz O, Koerver R, Braun P, Weber A, Ivers-Tiffée E, Adermann T, Kulisch J, Zeier WG, Richter FH, Janek J. *Nat Energy*, 2020, 5: 259–270
78 Zhang Q, Cao D, Ma Y, Natan A, Aurora P, Zhu H. *Adv Mater*, 2019, 31: 1901131
79 Meng X, Liu Y, Guan M, Qiu J, Wang Z. *Adv Mater*, 2022, 34: 2201981
80 Reinoso DM, Frechero MA. *Energy Storage Mater*, 2022, 52: 430–464
81 Huang WZ, Zhao CZ, Wu P, Yuan H, Feng WE, Liu ZY, Lu Y, Sun S, Fu ZH, Hu JK, Yang SJ, Huang JQ, Zhang Q. *Adv Energy Mater*, 2022, 12: 2201044
82 Paul PP, Chen BR, Langevin SA, Dufek EJ, Nelson Weker J, Ko JS. *Energy Storage Mater*, 2022, 45: 969–1001
83 Zhao CZ, Zhao BC, Yan C, Zhang XQ, Huang JQ, Mo Y, Xu X, Li H, Zhang Q. *Energy Storage Mater*, 2020, 24: 75–84
84 Zhang H, Chen Y, Li C, Armand M. *SusMat*, 2021, 1: 24–37
85 Wu L, Wang Y, Guo X, Ding P, Lin Z, Yu H. *SusMat*, 2022, 2: 264–292
86 Chai Y, Jia W, Hu Z, Jin S, Jin H, Ju H, Yan X, Ji H, Wan LJ. *Chin Chem Lett*, 2021, 32: 1139–1143
87 Weng W, Zhou D, Liu G, Shen L, Li M, Chang X, Yao X. *Mater Futures*, 2022, 1: 021001
88 Lv Q, Song Y, Wang B, Wang S, Wu B, Jing Y, Ren H, Yang S, Wang L, Xiao L, Wang D, Liu H, Dou S. *J Energy Chem*, 2023, 81: 613–622
89 Meng N, Zhu X, Lian F. *Particuology*, 2022, 60: 14–36
90 Jagger B, Pasta M. *Joule*, 2023, 7: 2228–2244
91 Lv F, Wang Z, Shi L, Zhu J, Edström K, Mindemark J, Yuan S. *J Power Sources*, 2019, 441: 227175
92 Yang X, Doyle-Davis K, Gao X, Sun X. *eTransportation*, 2022, 11: 100152
93 Kato Y, Shiotani S, Morita K, Suzuki K, Hirayama M, Kanno R. *J Phys Chem Lett*, 2018, 9: 607–613
94 Kalnaus S, Dudney NJ, Westover AS, Herbert E, Hackney S. *Science*, 2023, 381: 1300
95 Sun YZ, Huang JQ, Zhao CZ, Zhang Q. *Sci China Chem*, 2017, 60: 1508–1526
96 Zhao CZ, Duan H, Huang JQ, Zhang J, Zhang Q, Guo YG, Wan LJ. *Sci China Chem*, 2019, 62: 1286–1299
97 Wang Q, Dong T, Zhou Q, Cui Z, Shangguan X, Lu C, Lv Z, Chen K, Huang L, Zhang H, Cui G. *Sci China Chem*, 2022, 65: 934–942
98 Chang X, Zhao YM, Yuan B, Fan M, Meng Q, Guo YG, Wan LJ. *Sci China Chem*, 2023, DOI:10.1007/s11426-022-1525-3
99 Huang WZ, Liu ZY, Xu P, Kong WJ, Huang XY, Shi P, Wu P, Zhao CZ, Yuan H, Huang JQ, Zhang Q. *J Mater Chem A*, 2023, 11: 12713–12718
100 Liu Y, Zheng L, Gu W, Shen Y, Chen L. *Acta Physico Chim Sin*, 2021, 37: 2004058
101 Xiao Y, Xu R, Yan C, Liang Y, Ding JF, Huang JQ. *Sci Bull*, 2020, 65: 909–916
102 Zhou L, Zhao M, Chen X, Zhou J, Wu M, Wu N. *Sci China Chem*, 2022, 65: 1817–1821
103 Wang ZY, Zhao CZ, Sun S, Liu YK, Wang ZX, Li S, Zhang R, Yuan H, Huang JQ. *Matter*, 2023, 6: 1096–1124
104 Ma C, Cui W, Liu X, Ding Y, Wang Y. *InfoMat*, 2021, 4: e12232
105 Wang C, Sun J, Qu X, Liu X, Dong S, Cui G. *Curr Opin Electrochem*, 2022, 33: 100962
106 Su Y, Xu F, Zhang X, Qiu Y, Wang H. *Nano-Micro Lett*, 2023, 15: 82
107 Liu K, Zhang R, Sun J, Wu M, Zhao T. *ACS Appl Mater Interfaces*, 2019, 11: 46930–46937
108 Song Q, Zhang Y, Liang J, Liu S, Zhu J, Yan X. *Chin Chem Lett*, 2023, 34: 108797
109 Zhang X, Fu C, Cheng S, Zhang C, Zhang L, Jiang M, Wang J, Ma

Y, Zuo P, Du C, Gao Y, Yin G, Huo H. *Energy Storage Mater*, 2023, 56: 121–131
110 Dong P, Zhang X, Han KS, Cha Y, Song MK. *J Energy Chem*, 2022, 70: 363–372
111 Na Y, Chen Z, Xu Z, An Q, Zhang X, Sun X, Cai S, Zheng C. *Chin Chem Lett*, 2022, 33: 4037–4042
112 Huang X, Huang S, Wang T, Zhong L, Han D, Xiao M, Wang S, Meng Y. *Adv Funct Mater*, 2023, 33: 2300683
113 Wang H, Song J, Zhang K, Fang Q, Zuo Y, Yang T, Yang Y, Gao C, Wang X, Pang Q, Xia D. *Energy Environ Sci*, 2022, 15: 5149–5158
114 Sun M, Zeng Z, Zhong W, Han Z, Peng L, Cheng S, Xie J. *Batteries Supercaps*, 2022, 5: e202200338
115 Wang Y, Chen S, Li Z, Peng C, Li Y, Feng W. *Energy Storage Mater*, 2022, 45: 474–483
116 Wang HC, Cao X, Liu W, Sun X. *Front Energy Res*, 2019, 7: 112
117 Wang H, Wang Q, Cao X, He Y, Wu K, Yang J, Zhou H, Liu W, Sun X. *Adv Mater*, 2020, 32: 2001259
118 Chen T, Chen S, Chen Y, Zhao M, Losic D, Zhang S. *Mater Chem Front*, 2021, 5: 1771–1794
119 Yu P, Sun Q, Liu Y, Ma B, Yang H, Xie M, Cheng T. *ACS Appl Mater Interfaces*, 2022, 14: 7972–7979
120 Liu F, Bin F, Xue J, Wang L, Yang Y, Huo H, Zhou J, Li L. *ACS Appl Mater Interfaces*, 2020, 12: 22710–22720
121 Cheng X, Jiang Y, Lu C, Li J, Qu J, Wang B, Peng H. *Batteries Supercaps*, 2023, 6: e202300057
122 Chae W, Kim B, Ryoo WS, Earmme T. *Polymers*, 2023, 15: 803
123 Liang H, Wang L, Wang A, Song Y, Wu Y, Yang Y, He X. *Nano-Micro Lett*, 2023, 15: 42
124 Chang R, Liang Y, Hao Q, Xu J, Li N. *Chem Phys Lett*, 2023, 820: 140468
125 Guo C, Du K, Tao R, Guo Y, Yao S, Wang J, Wang D, Liang J, Lu SY. *Adv Funct Mater*, 2023, 33: 2301111
126 Yu Q, Jiang K, Yu C, Chen X, Zhang C, Yao Y, Jiang B, Long H. *Chin Chem Lett*, 2021, 32: 2659–2678
127 Lin Y, Shen Z, Huang J, Zhu J, Jiang S, Zhan S, Xie Y, Chen J, Shi Z. *J Power Sources*, 2023, 584: 233612
128 Wen W, Zeng Q, Chen P, Wen X, Li Z, Liu Y, Guan J, Chen A, Liu W, Zhang L. *Nano Res*, 2022, 15: 8946–8954
129 Zhang C, Zhang S, Zhang Y, Wu X, Lin L, Hu X, Wang L, Lin J, Sa B, Wei G, Peng DL, Xie Q. *Small Struct*, 2023, 4: 202300301
130 Liu W, Meng L, Liu X, Gao L, Wang X, Kang J, Ju J, Deng N, Cheng B, Kang W. *J Energy Chem*, 2023, 76: 503–515
131 Xiao G, Xu H, Bai C, Liu M, He YB. *Interdisciplinary Mater*, 2023, 2: 609–634
132 Liu Q, Wang L, He X. *Adv Energy Mater*, 2023, 13: 2300798
133 Duan H, Yin YX, Zeng XX, Li JY, Shi JL, Shi Y, Wen R, Guo YG, Wan LJ. *Energy Storage Mater*, 2018, 10: 85–91
134 Zhang SZ, Xia XH, Xie D, Xu RC, Xu YJ, Xia Y, Wu JB, Yao ZJ, Wang XL, Tu JP. *J Power Sources*, 2019, 409: 31–37
135 Zhou D, Shanmukaraj D, Tkacheva A, Armand M, Wang G. *Chem*, 2019, 5: 2326–2352
136 Nikodimos Y, Su WN, Taklu BW, Merso SK, Hagos TM, Huang CJ, Redda HG, Wang CH, Wu SH, Yang CC, Hwang BJ. *J Power Sources*, 2022, 535: 231425
137 Mu K, Wang D, Dong W, Liu Q, Song Z, Xu W, Yao P, Chen Y, Yang B, Li C, Tian L, Zhu C, Xu J. *Adv Mater*, 2023, 35: 2304686
138 Li Q, Zhang Z, Li Y, Li H, Liu Z, Liu X, Xu Q. *ACS Appl Mater Interfaces*, 2022, 14: 49700–49708
139 Sun M, Zeng Z, Peng L, Han Z, Yu C, Cheng S, Xie J. *Mater Today Energy*, 2021, 21: 100785
140 Liu Q, Yu Q, Li S, Wang S, Zhang LH, Cai B, Zhou D, Li B. *Energy Storage Mater*, 2020, 25: 613–620
141 Manthiram A, Yu X, Wang S. *Nat Rev Mater*, 2017, 2: 16103
142 Nair JR, Imholt L, Brunklaus G, Winter M. *Electrochem Soc Interface*, 2019, 28: 55–61
143 Peled E, Straze H. *J Electrochem Soc*, 1977, 124: 1030–1035
144 Warshawsky I. *J Electrochem Soc*, 1980, 127: 1324
145 Cheng XB, Zhang R, Zhao CZ, Wei F, Zhang JG, Zhang Q. *Adv Sci*, 2016, 3: 1500213
146 Li M, Lu J, Chen Z, Amine K. *Adv Mater*, 2018, 30: 1800561
147 Deiseroth HJ, Kong ST, Eckert H, Vannahme J, Reiner C, Zaiß T, Schlosser M. *Angew Chem Int Ed*, 2008, 47: 755–758
148 Kamaya N, Homma K, Yamakawa Y, Hirayama M, Kanno R, Yonemura M, Kamiyama T, Kato Y, Hama S, Kawamoto K, Mitsui A. *Nat Mater*, 2011, 10: 682–686
149 Kato Y, Hori S, Saito T, Suzuki K, Hirayama M, Mitsui A, Yonemura M, Iba H, Kanno R. *Nat Energy*, 2016, 1: 16030
150 Fu KK, Gong Y, Hitz GT, McOwen DW, Li Y, Xu S, Wen Y, Zhang L, Wang C, Pastel G, Dai J, Liu B, Xie H, Yao Y, Wachsman ED, Hu L. *Energy Environ Sci*, 2017, 10: 1568–1575
151 Liu FQ, Wang WP, Yin YX, Zhang SF, Shi JL, Wang L, Zhang XD, Zheng Y, Zhou JJ, Li L, Guo YG. *Sci Adv*, 2018, 4: eaat5383
152 Zhao Q, Liu X, Stalin S, Khan K, Archer LA. *Nat Energy*, 2019, 4: 365–373
153 Lin Y, Chen J, Zhu J, Zhong J, Yang K, Deng H, Huang J, Shen Z, Shi Z. *Surfs Interfaces*, 2023, 37: 102737
154 Chu Z, Zhuang S, Lu J, Li J, Wang C, Wang T. *Chin Chem Lett*, 2023, 34: 107563
155 Shen Z, Zhong J, Chen J, Xie W, Yang K, Lin Y, Chen J, Shi Z. *Chin Chem Lett*, 2023, 34: 107370
156 Amici J, Calderón CA, Versaci D, Luque G, Barraco D, Leiva E, Francia C, Bodoardo S. *Electrochim Acta*, 2022, 404: 139772
157 Zhang Y, Shi Y, Hu XC, Wang WP, Wen R, Xin S, Guo YG. *Adv Energy Mater*, 2019, 10: 1903325
158 Li SY, Wang WP, Xin S, Zhang J, Guo YG. *Energy Storage Mater*, 2020, 32: 458–464
159 Tan SJ, Yue J, Tian YF, Ma Q, Wan J, Xiao Y, Zhang J, Yin YX, Wen R, Xin S, Guo YG. *Energy Storage Mater*, 2021, 39: 186–193
160 Lin Z, Guo X, Wang Z, Wang B, He S, O'Dell LA, Huang J, Li H, Yu H, Chen L. *Nano Energy*, 2020, 73: 104786
161 Sun Z, Xi K, Chen J, Abdelkader A, Li MY, Qin Y, Lin Y, Jiang Q, Su YQ, Kumar RV, Ding S. *Nat Commun*, 2022, 13: 3209
162 Cao C, Li Y, Feng Y, Long P, An H, Qin C, Han J, Li S, Feng W. *J Mater Chem A*, 2017, 5: 22519–22526
163 Bouchet R, Maria S, Meziane R, Aboulaich A, Lienafa L, Bonnet JP, Phan TNT, Bertin D, Gigmes D, Devaux D, Denoyel R, Armand M. *Nat Mater*, 2013, 12: 452–457
164 Porcarelli L, Shaplov AS, Bella F, Nair JR, Mecerreyes D, Gerbaldi C. *ACS Energy Lett*, 2016, 1: 678–682
165 Zhang S, Sun F, Du X, Zhang X, Huang L, Ma J, Dong S, Hilger A, Manke I, Li L, Xie B, Li J, Hu Z, Komarek AC, Lin HJ, Kuo CY, Chen CT, Han P, Xu G, Cui Z, Cui G. *Energy Environ Sci*, 2023, 16: 2591–2602
166 Su Y, Rong X, Gao A, Liu Y, Li J, Mao M, Qi X, Chai G, Zhang Q, Suo L, Gu L, Li H, Huang X, Chen L, Liu B, Hu YS. *Nat Commun*, 2022, 13: 4181
167 Xie Z, Zhou Y, Ling C, Zhu X, Fang Z, Fu X, Yan W, Yang Y. *Chin Chem Lett*, 2022, 33: 1407–1411
168 Gao S, Li Z, Zhang Z, Li B, Chen XC, Yang G, Saito T, Tian M, Yang H, Cao PF. *Energy Storage Mater*, 2023, 55: 214–224
169 Guo K, Wang J, Shi Z, Wang Y, Xie X, Xue Z. *Angew Chem Int Ed*, 2023, 62: e202213606
170 Hu J, Wang W, Zhou B, Feng Y, Xie X, Xue Z. *J Membrane Sci*, 2019, 575: 200–208
171 Hwang SS, Cho CG, Kim H. *Electrochem Commun*, 2010, 12: 916–919
172 Nair JR, Shaji I, Ehteshami N, Thum A, Diddens D, Heuer A, Winter M. *Chem Mater*, 2019, 31: 3118–3133
173 Chen D, Zhu M, Kang P, Zhu T, Yuan H, Lan J, Yang X, Sui G. *Adv Sci*, 2021, 9: 2103663
174 Xiang J, Zhang Y, Zhang B, Yuan L, Liu X, Cheng Z, Yang Y, Zhang X, Li Z, Shen Y, Jiang J, Huang Y. *Energy Environ Sci*, 2021, 14: 3510–3521
175 Wen S, Luo C, Wang Q, Wei Z, Zeng Y, Jiang Y, Zhang G, Xu H,

Wang J, Wang C, Chang J, Deng Y. *Energy Storage Mater*, 2022, 47: 453–461
176 Zhu J, Zhang J, Zhao R, Zhao Y, Liu J, Xu N, Wan X, Li C, Ma Y, Zhang H, Chen Y. *Energy Storage Mater*, 2023, 57: 92–101
177 Cui Y, Chai J, Du H, Duan Y, Xie G, Liu Z, Cui G. *ACS Appl Mater Interfaces*, 2017, 9: 8737–8741
178 Zhou H, Liu H, Li Y, Yue X, Wang X, Gonzalez M, Meng YS, Liu P. *J Mater Chem A*, 2019, 7: 16984–16991
179 Meisner QJ, Jiang S, Cao P, Glossmann T, Hintennach A, Zhang Z. *J Mater Chem A*, 2021, 9: 25927–25933
180 Park S, Sohn JY, Hwang IT, Shin J, Yun JM, Eom KS, Shin K, Lee YM, Jung CH. *Chem Eng J*, 2023, 452: 139339
181 Wang Y, Qiu J, Peng J, Li J, Zhai M. *J Mater Chem A*, 2017, 5: 12393–12399
182 Li Q, Zhang X, Peng J, Wang Z, Rao Z, Li Y, Li Z, Fang C, Han J, Huang Y. *ACS Appl Mater Interfaces*, 2022, 14: 21018–21027
183 Zhang J, Zhou M, Shi J, Zhao Y, Wen X, Su CC, Wu J, Guo J. *Nano Energy*, 2021, 88: 106298
184 Lei X, Liu X, Ma W, Cao Z, Wang Y, Ding Y. *Angew Chem Int Ed*, 2018, 57: 16131–16135
185 Lu Z, Peng L, Rong Y, Wang E, Shi R, Yang H, Xu Y, Yang R, Jin C. *Energy Environ Mater*, 2023, 6: e12498
186 Ding J, Xu R, Yan C, Xiao Y, Liang Y, Yuan H, Huang J. *Chin Chem Lett*, 2020, 31: 2339–2342
187 Ge M, Zhou X, Qin Y, Liu Y, Zhou J, Wang X, Guo B. *Chin Chem Lett*, 2022, 33: 3894–3898
188 Utomo NW, Deng Y, Zhao Q, Liu X, Archer LA. *Adv Mater*, 2022, 34: 2110333
189 Zhao CZ, Zhao Q, Liu X, Zheng J, Stalin S, Zhang Q, Archer LA. *Adv Mater*, 2020, 32: e1905629
190 Geng Z, Huang Y, Sun G, Chen R, Cao W, Zheng J, Li H. *Nano Energy*, 2022, 91: 106679
191 Yang H, Zhang B, Jing M, Shen X, Wang L, Xu H, Yan X, He X. *Adv Energy Mater*, 2022, 12: 2201762
192 Zheng J, Zhang W, Huang C, Shen Z, Wang X, Guo J, Li S, Mao S, Lu Y. *Mater Today Energy*, 2022, 26: 100984
193 Wang A, Geng S, Zhao Z, Hu Z, Luo J. *Adv Funct Mater*, 2022, 32: 2201861
194 Chen X, Sun C, Wang K, Dong W, Han J, Ning D, Li Y, Wu W, Yang C, Lu Z. *J Electrochem Soc*, 2022, 169: 090509
195 Wu Y, Ma J, Jiang H, Wang L, Zhang F, Feng X, Xiang H. *Mater Today Energy*, 2023, 32: 101239
196 Duan H, Yin YX, Shi Y, Wang PF, Zhang XD, Yang CP, Shi JL, Wen R, Guo YG, Wan LJ. *J Am Chem Soc*, 2017, 140: 82–85
197 Duan H, Fan M, Chen WP, Li JY, Wang PF, Wang WP, Shi JL, Yin YX, Wan LJ, Guo YG. *Adv Mater*, 2019, 31: 1807789
198 Ma Q, Fu S, Wu AJ, Deng Q, Li WD, Yue D, Zhang B, Wu XW, Wang ZL, Guo YG. *Adv Energy Mater*, 2023, 13: 2203892
199 Lu J, Zhou J, Chen R, Fang F, Nie K, Qi W, Zhang JN, Yang R, Yu X, Li H, Chen L, Huang X. *Energy Storage Mater*, 2020, 32: 191–198
200 Wen J, Huang L, Huang Y, Luo W, Huo H, Wang Z, Zheng X, Wen Z, Huang Y. *Energy Storage Mater*, 2022, 45: 934–940
201 Tian JX, Guo HJ, Wan J, Liu GX, Wen R, Wan LJ. *Sci China Chem*, 2023, 66: 2921–2928
202 Cao W, Lu J, Zhou K, Sun G, Zheng J, Geng Z, Li H. *Nano Energy*, 2022, 95: 106983
203 Qiu J, Yang L, Sun G, Yu X, Li H, Chen L. *Chem Commun*, 2020, 56: 5633–5636
204 Chen K, Fang R, Lian Z, Zhang X, Tang P, Li B, He K, Wang D, Cheng HM, Sun Z, Li F. *Energy Storage Mater*, 2021, 37: 224–232
205 Ota H, Sakata Y, Otake Y, Shima K, Ue M, Yamaki J. *J Electrochem Soc*, 2004, 151: A1778
206 Hu Z, Zhang S, Dong S, Li W, Li H, Cui G, Chen L. *Chem Mater*, 2017, 29: 4682–4689
207 Wang G, Chen C, Chen Y, Kang X, Yang C, Wang F, Liu Y, Xiong X. *Angew Chem Int Ed*, 2019, 59: 2055–2060
208 Zhang QK, Zhang XQ, Wan J, Yao N, Song TL, Xie J, Hou LP, Zhou MY, Chen X, Li BQ, Wen R, Peng HJ, Zhang Q, Huang JQ. *Nat Energy*, 2023, 8: 725–735
209 Luo D, Zheng L, Zhang Z, Li M, Chen Z, Cui R, Shen Y, Li G, Feng R, Zhang S, Jiang G, Chen L, Yu A, Wang X. *Nat Commun*, 2021, 12: 186
210 Jin T, Liu M, Su K, Lu Y, Cheng G, Liu Y, Li NW, Yu L. *ACS Appl Mater Interfaces*, 2021, 13: 57489–57496
211 Xiong X, Qiao Q, Zhou Q, Cheng X, Liu L, Fu L, Chen Y, Wang B, Wu X, Wu Y. *Nano Res*, 2023, 16: 8448–8456
212 Sheng O, Jin C, Ju Z, Zheng J, Liu T, Liu Y, Wang Y, Luo J, Tao X, Nai J. *Nano Lett*, 2022, 22: 8346–8354
213 Sheng O, Zheng J, Ju Z, Jin C, Wang Y, Chen M, Nai J, Liu T, Zhang W, Liu Y, Tao X. *Adv Mater*, 2020, 32: 2000223
214 Hu R, Qiu H, Zhang H, Wang P, Du X, Ma J, Wu T, Lu C, Zhou X, Cui G. *Small*, 2020, 16: 1907163